MEASUREMENTS OF GAMMA-RAY SCATTERING USING A LIQUID-FILLED IONIZATION CHAMBER

N. E. WHITE AND W. B. HENDERSON

THESIS
W553

Library
U. S. Naval Postgraduate School
Monterey, California

MEASUREMENTS OF GAMMA-RAY SCATTERING USING A LIQUID-FILLED IONIZATION CHAMBER

by

NORMAN E. WHITE

B.S., U. S. Naval Academy
(1942)

and

WILLIAM B. HENDERSON

B.S., U. S. Naval Academy
(1944)

S.B., Massachusetts Institute of Technology
(1948)

SUBMITTED IN PARTIAL FULFILLMENT OF THE
REQUIREMENTS FOR THE DEGREE OF
MASTER OF SCIENCE

at the

MASSACHUSETTS INSTITUTE OF TECHNOLOGY
(1952)

Signature of Authors . . . . . .

. . . . . .
Department of Physics, May 16, 1952

Certified by . . . . . .
Thesis Supervisor

. . . . . .
Chairman, Departmental Committee on Graduate Students

Thesis
W553

ABSTRACT

Title: "Measurements of Gamma-Ray Scattering Using a Liquid-Filled Ionization Chamber"

Authors: Norman E. White and
William B. Henderson

Submitted to the Department of Physics on May 16, 1952 in partial fulfillment of the requirements for the degree of Master of Science.

18067

THESIS

Title: Measurements of Gamma-Ray Scattering Using a Lucite-Filled Ionization Chamber

Author: Thomas E. White USN

William E. Anderson

Submitted to the Department of Physics on May 16, 1950 in partial fulfillment of the requirements for degree of Doctor of Science.

18057

ABSTRACT

The instrument used in these measurements was the liquid-filled ionization chamber developed by M. A. VanDilla. Some modifications of the design of the chamber and the co-axial connection to the electrometer resulted in improved sensitivity, accuracy, and ease of use with no significant change in stability.

The scattering measurements were made using a Co^{60} source of about 3 mc activity. The scattering materials used were water, aluminum, iron, and lead. Two types of scattering from a semi-infinite medium were investigated: 1) side-scattering, in which the scattering medium was below and parallel to the plane of the source and detector; 2) back-scattering, with the source in contact with the surface of the scattering medium.

The back-scattering measurements indicate an increase in scattering with decreasing Z from lead to aluminum, with a decrease in scattering for water; the concept of an "image" source is developed to explain this effect.

The side-scattering measurements indicate that this effect is a strong and complex function of the atomic number of the scattering material, the separation

ABSTRACT

The instrument used in these measurements was the liquid-filled ionization chamber developed by E. A. Vandilla. Some modifications of the design of the chamber and the co-axial connection to the electrometer resulted in improved sensitivity, accuracy, and ease of use with no significant change in stability.

The scattering measurements were made using a Co^{60} source of about 3 mc activity. The scattering materials used were water, aluminum, iron, and lead. Two types of scattering from a semi-infinite medium were investigated: 1) side-scattering, in which the scattering medium was below and parallel to the plane of the source and detector; 2) back-scattering, with the source in contact with the surface of the scattering medium.

The back-scattering measurements indicate an increase in scattering with decreasing Z from lead to aluminum, with a decrease in scattering for water; the concept of an "image" source is developed to explain this effect.

The side-scattering measurements indicate that this effect is a strong and complex function of the atomic number of the scattering material, the superposition

of the source and detector, and the separation of the surface of the scattering medium from the plane of the source and the detector. Furthermore, the finite size of the detector has a considerable effect. Curves are presented illustrating these effects and qualitative explanations are offered.

Thesis Supervisor: Robley D. Evans

Title: Professor of Physics

of the source and detector, and the separation of the surface of the scattering medium from the plane of the source and the detector. Furthermore, the finite size of the detector has a considerable effect. Curves are presented illustrating these effects and qualitative explanations are offered.

Thesis Supervisor: Dudley D. Evans

Title: Professor of Physics

TABLE OF CONTENTS

		Page
Section I.	Introduction.	
A.	Statement of Problem	1
B.	Introductory Remarks	1
Section II.	The Ionization Chamber.	
A.	Construction	3
B.	Electrical Circuit	6
C.	Theoretical Basis	15
D.	Characteristics of the Decane-Filled Chamber	20
Section III.	Penetration of γ-Rays through a Medium.	
A.	γ-Ray Interactions	34
B.	Review of Previous Studies of γ-Ray Penetration	37
Section IV.	Experimental Results.	
A.	Procedure	48
B.	Results	50
C.	Interpretation of Results; Comparison with Scattering in an Infinite Medium	57
Acknowledgments		74
Bibliography		75

TABLE OF CONTENTS

Page

Section I. Introduction.

A. Statement of Problem 1

B. Introductory Remarks 3

Section II. The Invariables Chamber.

A. Construction 8

B. Illustrated Step-by-Step 8

C. Conventional Tasks 12

D. Characteristics of the Chamber-Filled Number 20

Section III. Construction of x-step Sequence Tables.

A. x-Step Determinations 31

B. Series of Two-Place Studies of x-Step Permutation 37

Section IV. Convergent Results.

A. Procedure 49

B. Charts 50

C. Interpretation of Graphical Comparison with Derivation 57

Bibliography 73

I. INTRODUCTION

A. Statement of Problem

The object of this thesis is to investigate the problem of multiple γ-ray scattering from various semi-infinite media using a liquid-filled ionization chamber. Experimental results can be compared with those obtained by other investigators studying scattering in infinite media in the hope that a correlation may be obtained which will permit the use of results from experiments with semi-infinite media in the prediction of scattering effects in infinite media. This would greatly facilitate the study of multiple scattering in solid materials if adequate correlation can be obtained.

B. Introductory Remarks

Investigation of the effects of multiple scattering of γ-rays in infinite solid media is handicapped by the necessity of using large masses of material and boring holes in the material in order to place the source and detector inside the medium. This results in perturbations of the medium which may be of considerable importance in the case of heavy materials in which

I. INTRODUCTION

A. Statement of Problem

The object of this thesis is to investigate the problem of multiple γ-ray scattering from various semi-infinite media using a liquid-filled ionization chamber. Experimental results can be compared with those obtained by other investigators studying penetrating semi-infinite media in the hope that a correlation may be obtained which will permit the use of results from experiments with semi-infinite media in the prediction of scattering effects in infinite media. This would greatly facilitate the study of multiple scattering in solid materials if adequate correlation can be obtained.

B. Introductory Remarks

Investigation of the effects of multiple scattering of γ-rays in infinite solid media is handicapped by the necessity of using large masses of material and boring holes in the material in order to place the source and detector inside the medium. This results in perturbations of the medium which may be of considerable importance in the case of heavy materials in which

photons have short mean free paths. Furthermore, the experimental set-up is complex and unwieldy. It would be desirable to establish a correlation between experimental results obtained using infinite and semi-infinite media in order to facilitate studies over a wider range of materials in order to obtain experimental data on the effect of atomic number on multiple γ-ray scattering. To this end we investigate scattering from semi-infinite water and aluminum media and compare the results with those obtained by White[1] and VanDilla[2] using an infinite water medium and those of Gray[3] using an infinite aluminum medium and attempt to establish the desired correlation. If successful the results could then be applied to data obtained from iron and lead as well.

photons have short mean free paths. Furthermore, the experimental set-up is complex and unwieldy. It would be desirable to establish a correlation between experimental results obtained using infinite and semi-infinite media in order to facilitate studies over a wider range of materials in order to obtain experimental data on the effect of atomic number on multiple γ-ray scattering. To this end we investigate scattering from semi-infinite water and aluminum media and compare the result with those obtained by White[1] and Trubitt[2] using an infinite water medium and those of Grey[3] using an infinite aluminum medium and attempt to establish the desired correlation. If successful the results could then be applied to data obtained from iron and lead as well.

II. THE IONIZATION CHAMBER

A. Construction

The decane-filled ionization chamber which was used to measure the effect of γ-ray scattering by various materials is shown in Fig. 1. With the exception of the shell this is the same chamber which was designed by M. A. VanDilla,[2] who has described some of its characteristics and has used it to measure the penetration and diffusion of γ-rays in a large water medium.

The chamber is constructed entirely of lucite, except the two Teflon (tetrafluoroethylene polymer) insulators. Teflon, according to the manufacturer, E. I. DuPont de Nemours and Co., has a surface resistivity of 3.6×10^{12} ohms and a volume resistivity of 10^{16} ohms at 100 percent relative humidity. Surface contact between the horizontal surfaces of the insulators and the lucite is minimized by the bevel in the lucite surfaces. The entire center electrode, the inside surface of the guard-ring section, and the inside surface and top edge of the shell are made electrically conducting by painting with Aquadag, one of the several dispersions of colloidal graphite made by the Acheson Colloids

II. THE IONIZATION CHAMBER

A. Construction

The dense-filled ionization chamber which was used to measure the effect of γ-ray scattering by various materials is shown in Fig. 1. With the exception of the shell this is the same chamber which was designed by H. A. Wright,[3] who has described some of its characteristics and has used it to measure the penetration and diffusion of γ-rays in a large water medium.

The chamber is constructed entirely of Lucite, except the two Teflon (tetrafluoroethylene polymer) insulators. Teflon, according to the manufacturer, E. I. DuPont de Nemours and Co., has a surface resistivity of 8.6×10^{12} ohms and a volume resistivity of 10^{16} ohms at 100 percent relative humidity. Surface contact between the horizontal surfaces of the insulators and the Lucite is minimized by the bevel in the Lucite surfaces. The entire center electrode, the inside surface of the guard-ring section, and the inside surface and top edge of the shell are made electrically conductive by painting with Aquadag, one of the several dispersions of colloidal graphite made by the Acheson Colloids

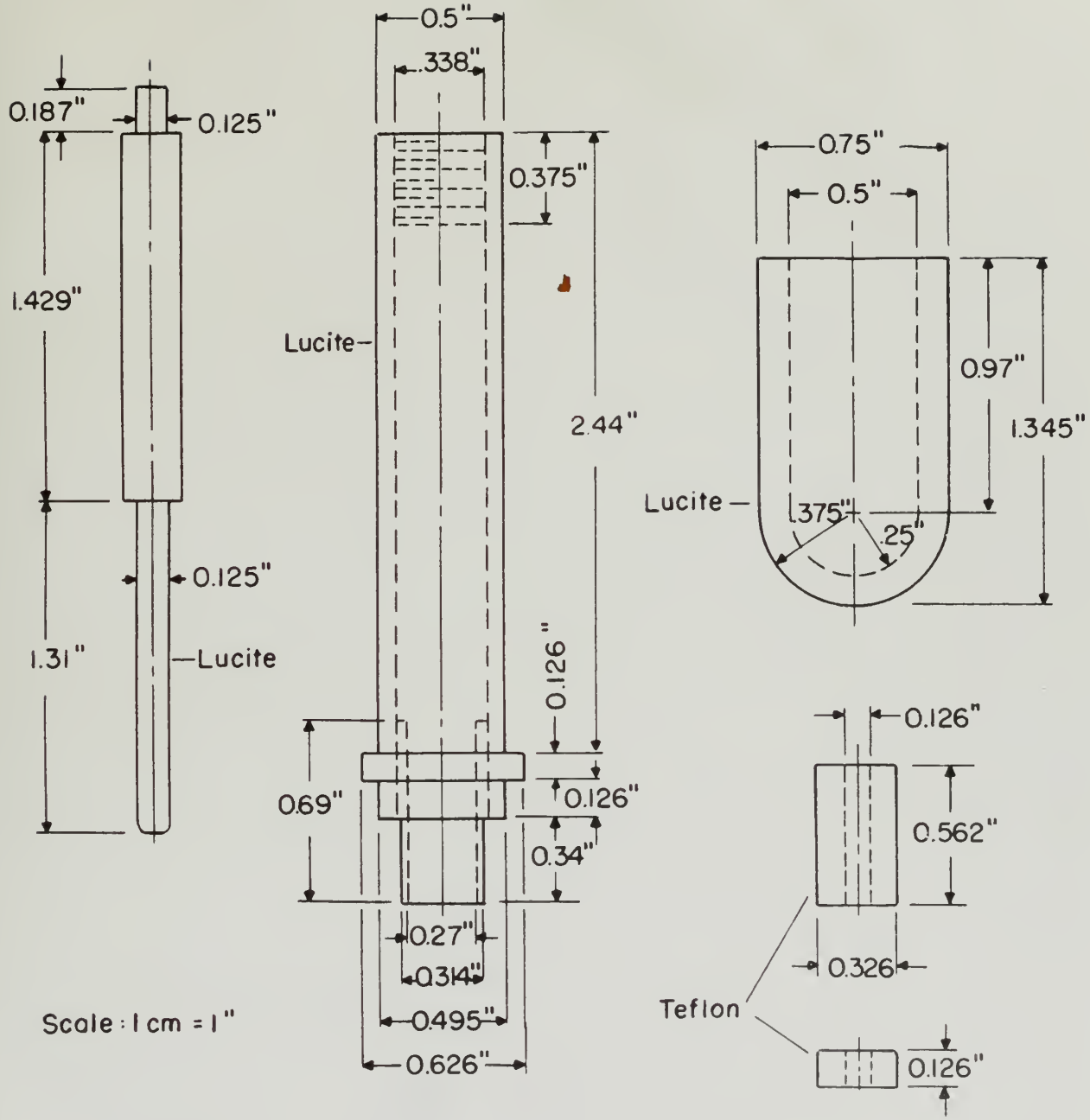

COMPONENT PARTS OF LIQUID FILLED IONIZATION CHAMBER

Figure 1

Corporation. Considerable care is necessary to obtain a coating over the sharp edges of the bevelled surfaces.

Since Aquadag chips off easily, several other dispersions were tried. Dag Dispersion No. 194, which contains a lacquer solvent and a binding agent, was found to produce a low resistance coating which did not chip off readily; but decane attacks the binder to the extent that the coating can be wiped off with little effort. For fear that the decane filling would become contaminated with colloidal graphite and exhibit excessive conductivity, the use of Dag No. 194 was restricted to the threaded portion of the guard-ring section, where maximum adhesion of the coating is needed.

Lucite is chemically resistant to decane and to toluene, the solvent used to remove Dag No. 194, whereas polystyrene, which is almost identical with lucite in physical appearance, is softened almost immediately by toluene. VanDilla reports that polystyrene slowly swells when in contact with decane, hence his use of lucite for the chamber parts; however his shell which we replaced was attacked by toluene.

The initial reasons for replacing the shell were 1) that the center electrode extended well below the cen-

1) that the center electrode extended well below the com-

The limited reasons for replacing the shell were

was attacked by toluene.

when in contact with decane, hence its use of Lucite for

volume. Vendilla reports that polystyrene slowly swells

physical appearance, it softened almost immediately by

polystyrene, which is almost identical with Lucite in

toluene, the solvent used to remove Dwg No. 194, whereas

Lucite is chemically resistant to decane and to

The unthreaded portion of the ground-ring section, where maxi-

mum adhesion of the coating is needed.

ductivity, the use of Dwg No. 191 was restricted to the

ted with colloidal graphite and exhibit excessive con-

for fear that the decane filling would become contamina-

tent that the coating can be wiped off with little effort.

to produce a low resistance coating which did not only

off readily; but became attacks the binder to the ex-

tains a lacquer solvent and a binding agent, was found

perations were tried. Dwg Dispersion No. 191, which con-

Since dipping chips off easily, several other dis-

a coating over the sharp edges of the beveled sur-

face.

Corporation. Considerable care is necessary to obtain

ter of curvature of the spherical portion and 2) that the shell had been left filled with radioactive decane, which was used by VanDilla in an attempt to obtain an absolute calibration of decane-filled ionization chamber. The new shell has a sensitive volume of about 2 cc and a wall thickness of 1/8".

B. Electrical Circuit

The electrical circuit and the electronic components which are used with the ionization chamber are shown schematically in Fig. 2. An electrode for applying a collecting voltage across the shell is made by inserting a thin strip of aluminum foil around the inside of the shell at the top, with a projection sticking out for attaching a clip-lead from the battery bank. The shell can then be slipped onto the guard-ring section, and the mechanical fit is tight enough to hold the shell in place. A film of paraffin is deposited over the joint to inhibit evaporation of the decane filling. The lower Teflon insulator acts to seal off the shell internally.

The instrument used to measure current output of the chamber is a vibrating-reed electrometer[4] made by the Applied Physics Corporation, Pasadena, California.

ter of curvature of the spherical portion and 2) that the shell had been left filled with radioactive decane, which was used by Tantilla in an attempt to obtain an absolute calibration of decane-filled ionization chamber. The new shell has a sensitive volume of about 2 cc and a wall thickness of 1/8".

3. Electrical Circuit

The electrical circuit and the electronic components which are used with the ionization chamber are shown schematically in Fig. 3. An electrode for applying a collecting voltage across the shell is made by inserting a thin strip of aluminum foil around the inside of the shell at the top, with a projection sticking out for attaching a clip-lead from the battery bank. The shell can then be slipped onto the quartz-ring section, and the mechanical fit is tight enough to hold the shell in place. A film of paraffin is deposited over the joint to inhibit evaporation of the decane filling. The lower Teflon insulator acts to seal off the shell internally.

The instrument used to measure current output of the chamber is a vibrating-reed electrometer[4] made by the Applied Physics Corporation, Pasadena, California.

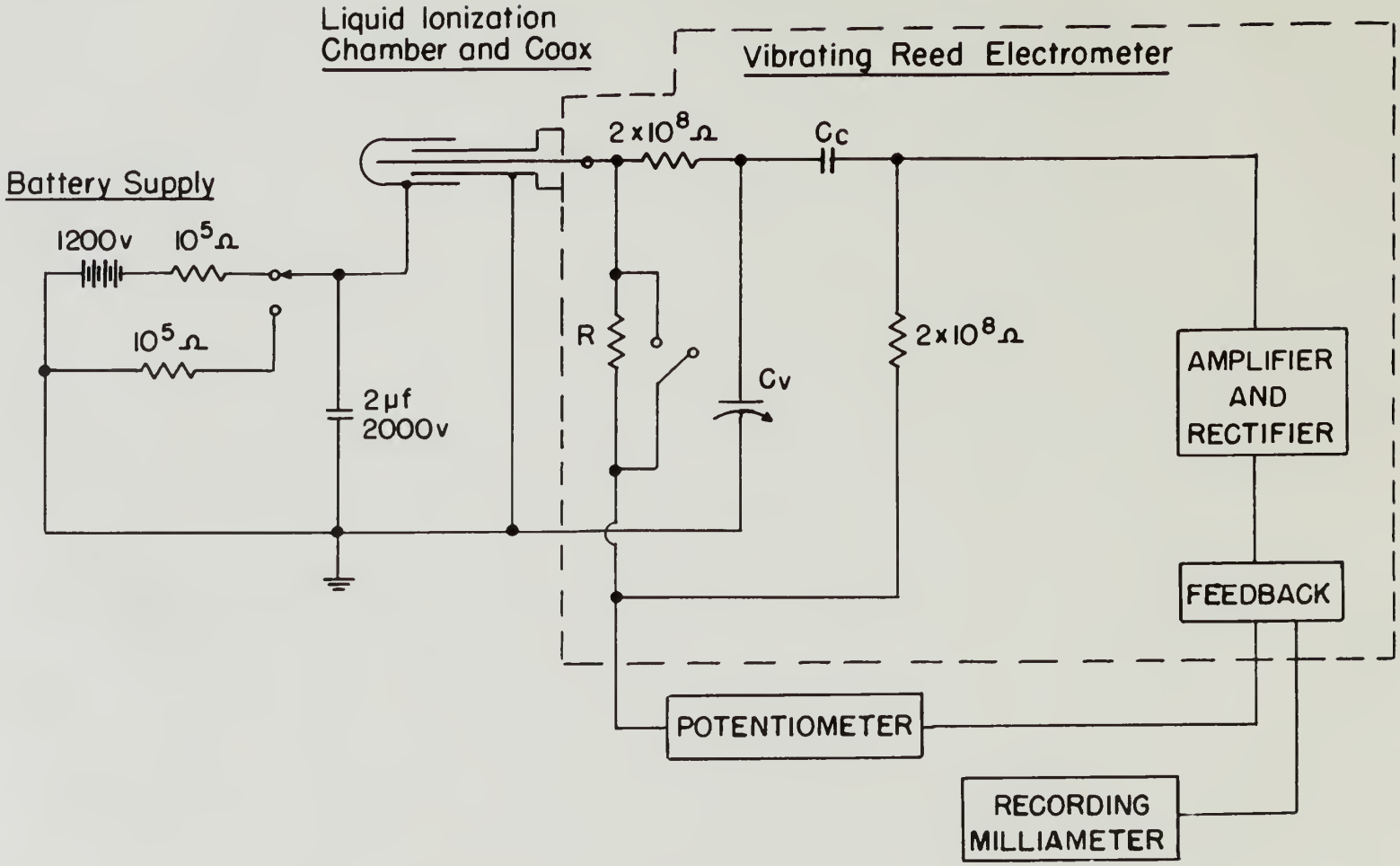

CIRCUIT USED WITH LIQUID ION CHAMBER

Figure 2

This instrument consists of 1) a head amplifier unit, containing a vibrating-reed capacitor, C_v, driven by the output of a Wien-bridge oscillator and 2) an amplifier-rectifier unit. Whenever a charge, Q, exists on the capacitor C_v, the variation in capacitance produces an alternating voltage at a frequency of about 450 c.p.s. This voltage is amplified and is rectified by means of a synchronous rectifier. A d-c output voltage, V, is produced at the cathode of a cathode follower, and a voltage divider network is used to apply a portion, V_f, of the output voltage to one side of capacitor C_c, and opposite in polarity to the d-c voltage on C_v. The initial charge, Q, divides between C_v and C_c so that

$$\frac{Q'}{C_v} - \frac{Q''}{C_c} = - \frac{AQ'}{C_v} = V_f$$

where A is the amplification of the system. Then

$$Q = Q' + Q'' = V_f \left[C_c \frac{(A + 1)}{A} + \frac{C_v}{A} \right] .$$

A is about 1000 and C_v and C_c are 25 μμf and 10 μμf respectively. Thus Q is practically independent of the actual value of A and is approximately $C_c V_f$.

In order to measure currents less than about 10^{-15} amps, the rate of charge method is used; but for larger currents a more convenient method is to use the resistor

This instrument consists of 1) a tuned amplifier unit, containing a vibrating-reed capacitor, C^v, driven by the output of a Wien-bridge oscillator and 2) an amplifier-rectifier unit. Whenever a charge, q, exists on the capacitor C^v, the variation in capacitance produces an alternating voltage at a frequency of about 450 c.p.s. This voltage is amplified and is rectified by means of a synchronous rectifier. A d-c output voltage, V, is produced at the cathode of a cathode follower, and a voltage divider network is used to apply a portion, V', of the output voltage to one side of capacitor C^c, and opposite in polarity to the d-c voltage on C^v. The initial charge, q, divides between C^v and C^c so that

$$\frac{q'}{C^v} - \frac{q_m}{C^c} = -\frac{\Delta C'}{C^v} = V'$$

where A is the amplification of the system. Then

$$q = q' + q_m = V'\left[C^c\,\frac{(A+1)}{A} + \frac{C^v}{A}\right] .$$

A is about 1000 and C^v and C^c are 25 μμf and 10 μμf respectively. Thus q is practically independent of the actual value of A and is approximately C^cV'.

In order to measure currents less than about 10^{-13} amps, the rate of charge method is used; but for larger currents a more convenient method is to use the resistor

R and record the output voltage as a trace on the recorder chart. In the course of these experiments only the latter method was used. The resistor R is a Victoreen high-meg resistor of about 10^{11} ohms. The trace on the Esterline-Angus recorder is a record of the instantaneous current, and the statistical average can be estimated by observing the trace over the period of the measurement. When a steady current I flows into the electrometer, a steady state is reached, and all the current flows through resistor R and the feedback network to ground. Since 10^{11} ohms is very much greater than the resistance in the feedback network,

$$IR + V_f = \frac{Q'}{C_v} = -\frac{V_f}{A} \quad \text{and} \quad IR = -V_f\left(\frac{A+1}{A}\right) = -V_f \ .$$

The electrometer reads "up scale" when the shell is negative with respect to the center electrode.

The resistance network in the cathode circuit of the cathode follower consists of two branches, one of which contains the voltage divider network and the other, which contains the electrometer milliammeter and calibrating rheostat. The recording milliammeter is inserted in series with the latter, and the rheostat is adjusted by comparing the milliammeter readings with the voltage from the potentiometer inserted in series with

3 and record the output voltage as a trace on the recorder chart. In the course of these experiments only the latter method was used. The resistor R is a Victoreen high-meg resistor of about 10^{11} ohms. The trace on the Esterline-Angus recorder is a record of the instantaneous current, and the statistical average can be estimated by observing the trace over the period of the measurement. When a steady current I flows into the electrometer, a steady state is reached, and all the current flows through resistor R and the feedback network to ground. Since 10^{11} ohms is very much greater than the resistance in the feedback network,

$$IR + V_1 = \frac{Q_1}{C_v} = -\frac{1}{A}V_2 \quad \text{and} \quad IR = -V_1\left(\frac{A+1}{A}\right) = -V_2 \ .$$

The electrometer reads "up scale" when the shell is negative with respect to the center electrode.

The resistance network in the cathode circuit of the cathode follower consists of two branches, one of which contains the voltage divider network and the other, which contains the electrometer milliammeter and oscillating rheostat. The recording milliammeter is inserted in series with the latter, and the rheostat is adjusted by comparing the milliammeter readings with the voltage from the potentiometer inserted in series with

the feedback network. Both milliammeters have a full-scale deflection of 1 ma. Full scale deflections of 1 mv, 10 mv, 100 mv, and 1000 mv are obtained by taking the feedback voltage, V_f, from four positions on the voltage divider. When the feedback voltage is increased by a factor of 10, the gain of one of the amplifier stages is reduced by a factor of 10, keeping the overall gain constant.

Since it is difficult to read the scale of the recorder with a precision better than about 0.5 percent of full scale, a precision potentiometer made by the Rubicon Co. of Philadelphia is used to apply a known voltage in series with the feedback voltage. The voltage IR can be balanced out with an accuracy of about 0.4 percent by this method, and small changes can be read conveniently from the recorder trace with a precision which is theoretically 0.5 percent of the full-scale deflection chosen. Actually a point of diminishing returns may be reached as the full-scale deflection is decreased because of the fluctuations in current. A 3v battery supply in the potentiometer is balanced against a standard cell, and the output voltage is continuously variable from zero to about 1600 mv. Since only the small current from the ionization chamber flows in the

the feedback method. Both milliameters have a full-
scale deflection of 1 ma. Full scale deflections of
1 mv, 10 mv, 100 mv, and 1000 mv are obtained by taking
the feedback voltage, V_f, from four positions on the
voltage divider. When the feedback voltage is increased
by a factor of 10, the gain of one of the amplifier
stages is reduced by a factor of 10, keeping the overall
gain constant.

Since it is difficult to read the scale of the re-
corder with a precision better than about 0.5 percent
of full scale, a precision potentiometer made by the
Rubicon Co. of Philadelphia is used to apply a known
voltage in series with the feedback voltage. The vol-
tage IF can be balanced out with an accuracy of about
0.1 percent by this method, and small changes can be read
conveniently from the recorder trace with a precision
which is theoretically 0.5 percent of the full-scale
deflection chosen. Actually a point of diminishing re-
turns may be reached as the full-scale deflection is de-
creased because of the fluctuations in current. A dry
battery supply in the potentiometer is balanced against
a standard cell, and the output voltage is continuously
variable from zero to about 1600 mv. Since only the
small current from the ionization chamber flows in the

feedback loop when the current is constant, the potentiometer operates under essentially no load, as it must for its calibration to be correct.

The head amplifier unit should not be subjected to strong penetrating radiation, because some of the ions produced in the relatively large air spaces in the head are collected and constitute a background current. To avoid the necessity of shielding the head a 15" length of coax is used to connect the chamber to the head amplifier unit. This unit is mounted to the under side of a wooden stand so that the bottom of the chamber is about 60 cm from the floor. As originally used by Van Dilla, this coax consisted of an outer tube of aluminum alloy and an inner conductor of the same material held in place by two Teflon insulators. Although the center electrode is never at a potential of more than 1 mv with respect to ground by virtue of the feedback circuit, there are contact potentials between the inner and outer conductors which collect ions produced in the air spaces. To avoid these spurious currents as much as possible, we replaced the inner conductor of the coax with a stiff tungsten wire sealed into an evacuated section of pyrex tubing. The glass tubing fits snugly inside the outer aluminum conductor, and insulation between

feedback loop when the current is constant, the potentiometer operates under essentially no load, as it must for the calibration to be correct.

The head amplifier unit should not be subjected to strong penetrating radiation, because some of the ions produced in the relatively large air spaces in the head are collected and constitute a background current. To avoid the necessity of shielding the head a 10" length of coax is used to connect the chamber to the head amplifier unit. This unit is mounted to the under side of a wooden stand so that the bottom of the chamber is about 6½ cm from the floor. As originally used by Van Dilla, this coax consisted of an outer tube of aluminum alloy and an inner conductor of the same material held in place by two Teflon insulators. Although the center electrode is never at a potential of more than 1 mv with respect to ground by virtue of the feedback circuit, there are contact potentials between the inner and outer conductors which collect ions produced in the air space. To avoid these spurious currents as much as possible, we replaced the inner conductor of the coax with a stiff tungsten wire sealed into an evacuated section of pyrex tubing. The glass tubing fits snugly inside the outer aluminum conductor, and insulation between

inner and outer conductor is obtained by the tapered glass seals at each end of the glass tube. A spring-loaded contactor in the head amplifier unit makes contact with the tungsten wire through two flat brass discs, one of which is soldered to each of the contacting parts. Contact at the chamber between the tungsten wire and the center electrode is achieved by having the ends of each conductor enter the upper Teflon insulator far enough to compress a small metal spring. Electrical continuity is maintained between the case of the head amplifier and the guard-ring section through a brass cup which slips into the head and to which the aluminum tube is threaded and through the threaded aluminum-to-graphite joint at the guard-ring section. Shielding is thus obtained all the way to the sensitive volume of the shell, and a minimum air volume is achieved by the evacuated coax and the large body of the center electrode, which nearly fills the guard-ring section.

The ground terminal of the battery bank is connected to the case of the head amplifier. Shielding of the high voltage lead to the electrode at the shell is obtained by enclosing the batteries in a metal box and using a shielded lead to the shell. The purpose of the RC network across the battery bank is to reduce battery

noise, but removal of this network has no noticeable effect when the batteries are new. The battery bank consists of 300v Eveready No. 493 "B" batteries, with a switch providing two combinations of batteries at either positive or negative polarity with respect to ground.

C. Theoretical Basis

In order to understand why one might expect the response of the decane-filled ionization chamber, in terms of the current obtained by collecting the ions produced when the chamber is irradiated with a γ-ray flux, to be proportional under certain conditions to the dosage rate in roentgens per unit time at the position of the chamber, we must discuss the definition of the roentgen and the characteristics that an instrument must have in order to measure this quantity.

The roentgen is defined as "that quantity of X- or γ-radiation such that the associated corpuscular emission per 0.001293 gm of air produces, in air, ions carrying 1 electrostatic unit of quantity of electricity of either sign", where 0.001293 gm of air is the mass of 1 cc of dry air at 0°C and 760 mm Hg. This definition, like the definition of the inch and the foot, was made not because one is particularly interested in the substance

upon which the definition is based, in this case, air, but because it defines a quantity closely related to the actual one of interest, in this case energy per gram delivered to living tissue, and which can be measured to a sufficient degree of accuracy to be meaningful. The choice of air was made because it resembles soft tissue in atomic composition and is a convenient medium in which to make measurements.

Several consequences of the definition are immediately apparent. In order to measure this quantity a small enough volume of air must be chosen so that the radiation is constant over the volume, and all the ions produced in an infinite medium of air by the corpuscular radiations from this volume must be collected. Although these conditions are never satisfied completely in practice, close approximations can be obtained if the photon energy is not too high. At energies less than several hundred kev the "associated corpuscular radiation" is secondary electrons whose ranges are small enough that a "free-air" ionization chamber can be used. At higher energies the so-called "air-wall" ionization chambers are used. Kaye and Binks,[5] and more recently Taylor,[6] have described these instruments and their limitations.

The theoretical basis for the air-wall ionization

chamber was developed by Bragg,[7] Gray,[8] and others, but it was Gray who put this technique for measuring dosage on a sound theoretical and experimental basis, and it is stated mathematically by the Bragg-Gray Law,

$$\Delta E = JW\rho ,$$

where ΔE = γ-ray energy absorption/cc of absorbing medium/sec,

J = number of ion pairs formed/cc/sec in a small gas-filled cavity in the absorbing medium,

W = average energy expended per ion pair in the gas,

ρ = stopping power of the medium relative to the gas for secondary electrons.

The validity of this law depends on the fact that when a homogeneous medium is uniformly irradiated, the introduction of a small cavity into the medium leaves the atmosphere of electrons unchanged provided the range of the electrons in the cavity is much greater than the dimensions of the cavity. The value of W changes very little with the nature and energy of the ionizing radiation and with the nature of the medium being ionized. The value of ρ is also relatively independent of energy.

chamber was developed by Greig,[7] Gray,[8] and others, but it was Gray who put this technique for measuring dosage on a sound theoretical and experimental basis, and it is stated mathematically by the Gregg-Gray Law,

$$\Delta\Sigma = 1m\delta\,,$$

where $\Delta\Sigma$ = γ-ray energy absorption/cc of absorbing medium/sec,

1 = number of ion pairs formed/cc/sec in a small gas-filled cavity in the absorbing medium,

m = average energy expended per ion pair in the gas,

δ = stopping power of the medium relative to the gas for secondary electrons.

The validity of this law depends on the fact that when a homogeneous medium is uniformly irradiated, the introduction of a small cavity into the medium leaves the atmosphere of electrons unchanged provided the range of the electrons in the cavity is much greater than the dimensions of the cavity. The value of δ changes very little with the nature and energy of the ionizing radiation and with the nature of the medium being ionized. The value of δ is also relatively independent of energy.

The thickness of wall material of a chamber which most nearly approximates the conditions required for the validity of the Bragg-Gray Law is that thickness at which the primary photons have just reached equilibrium with the secondary electrons. If the wall material has the same atomic composition as air, then the current obtained by collecting the ions formed in the gas-filled cavity will be a direct measure of the dosage rate, since at equilibrium the walls approximate an infinite air medium and the number of ions produced per unit volume is equal to the number of ions produced by secondary electrons originating in a unit volume. Mayneord and Roberts,[9] using small graphite-wall chambers of various thicknesses, found that the maximum ionization current produced by γ-rays of RaB+C occurred at a wall thickness of about 4 mm, with a variation of less than 1 percent from 2 mm to 6 mm. The build-up of ionization current with wall thickness resembles the build-up of daughter activity with time in radioactive decay, because the mean range of the primary photons and of the secondary electrons is analogous to the mean life of the parent and of the daughter in radioactive decay. Since the mean range for photons is much greater than for the secondary electrons, equilibrium is reached at a wall

thickness of about the maximum range of the secondary electrons. The wall thickness must of course be great enough to prevent ionizing particles which originate outside the walls from reaching the cavity.

The question of whether or not the attenuation of the photon flux by the chamber should be corrected for depends on how much attenuation would have occurred in the medium in the absence of the chamber. When absolute values of dosage rate are desired in air, this correction may be appreciable. In the case of the 4 mm wall thickness Mayneord and Roberts found a 1.7 percent correction was required. In a medium such as tissue, where the attenuation is much greater than in air, an air-wall chamber filled with an air-equivalent material such that the attenuation by the chamber was about the same as by the original tissue would require a negligible correction to read the average dosage rate over that volume.

This is the motivation for the decane-filled chamber. When the lucite shell is filled with decane, a close approximation to a soft tissue medium is obtained. We used this chamber in our scattering measurements because its sensitivity is about 30 times that of an air-filled chamber of the same volume, enabling the use

I

of a chamber of small volume without requiring large source strengths which are inconvenient to obtain and to handle safely. The 1/8" lucite walls have a thickness of 0.375 g/cm^2, while the maximum range of secondary electrons is about 0.45 g/cm^2 (10) from the primary γ-rays of Co^{60}, which was the source used in all the scattering experiments. Both lucite and decane are essentially air-equivalent materials, so that in the sensitive volume of the chamber the number of ions produced per second is proportional to the average dosage rate in that volume. Unfortunately in liquids and solids it is never possible to collect all the ions formed; however if we could always collect a constant fraction of these ions, the output current from the chamber would be proportional to dosage rate. This proves to be the case if the γ-ray energy is not too low and the flux not too high.

In liquids such as decane free electrons probably are quickly attached to neutral molecules, and the ion current consists mainly of positively and negatively charged molecules. The mean free paths will be very short, and the ions will acquire little energy in excess of thermal energy. Some of the ions will be lost by recombination, and this process can be divided into two

general types: 1) initial recombination of ions formed along the track of a single ionizing particle, and 2) general recombination of ions from different tracks as the ions migrate due to their thermal motion and to the influence of the collecting field.

Lea[11] has shown that the ions along the path of an energetic, light, ionizing particle such as an electron form clusters along the path, and that the fraction of ions produced which recombine by initial recombination will be independent of the energy of the ionizing particle. The large field strengths in these clusters precludes an appreciable effect of the applied field. As the electron energy decreases, the separation of these clusters decreases, and eventually they will overlap before much diffusion of ions can take place. The columnar theory of Jaffe[12] then applies, and the fractional initial recombination is shown to depend on the energy of the ionizing particle. In air at 100 atmospheres pressure this effect occurs at about 1 Mev for electrons.

VanDilla has treated the diffusion equation which describes the general recombination in plane geometry. The fractional general recombination is found to be proportional to d^2/E^2, where d is the electrode separation and E is the applied field strength.

general types: 1) initial recombination of ions formed along the track of a single ionizing particle, and 2) general recombination of ions from different tracks as the ions migrate due to their thermal motion and to the influence of the collecting field.

Loeb[11] has shown that the ions along the path of an energetic, light, ionizing particle such as an electron form clusters along the path, and that the fraction of ions produced which recombine by initial recombination will be independent of the energy of the ionizing particle. The large field strengths in these clusters preclude an appreciable effect of the applied field. As the electron energy decreases, the separation of these clusters decreases, and eventually they will overlap before much diffusion of ions can take place. The columnar theory of Jaffe[12] then applies, and the fractional initial recombination is known to depend on the energy of the ionizing particle. In air at 100 atmospheres pressure this effect occurs at about 1 Mev for electrons.

Vandiia has treated the diffusion equation which describes the general recombination in plane geometry. The fractional general recombination is found to be proportional to d^2/E^2, where d is the electrode separation and E is the applied field strength.

D. Characteristics of the Decane-Filled Chamber

1. Wavelength response

Using several γ-ray sources and an X-ray source, VanDilla was able to obtain a wavelength response curve for the decane-filled chamber. This was done by comparing the response of the decane-filled chamber with that of the air-filled chamber for each source. The results show that the decane-filled chamber has a response independent of photon energy from about 3.0 Mev to 400 kev. Below 400 kev the response falls off, and is about 85 percent at 200 kev. This behavior indicates that the cluster theory of Lea is indeed applicable to the decane filling. Although we used a collecting voltage of 1200v, while VanDilla used 600v, we would expect no appreciable improvement in the wavelength response.

2. Temperature response

VanDilla obtained a temperature response curve which increases at about 0.8 percent per ^{o}C from about 10^{o}C to 40^{o}C. Although we did not repeat this measurement, we found that the ambient temperature variation of several degrees during the daytime made it difficult to obtain reliable data in the scattering experiments. All

D. Characteristics of the Decane-Filled Chamber

1. Wavelength response

Using several γ-ray sources and an X-ray source, Yamtilla was able to obtain a wavelength response curve for the decane-filled chamber. This was done by comparing the response of the decane-filled chamber with that of the air-filled chamber for each source. The results show that the decane-filled chamber has a response independent of photon energy from about 5.0 Mev to 400 kev. Below 400 kev the response falls off, and is about 85 percent at 200 kev. This behavior indicates that the cluster theory of Lea is indeed applicable to the decane filling. Although we used a collecting voltage of 1400v, while Yamtilla used 500v, we would expect no appreciable improvement in the wavelength response.

2. Temperature response

Yamtilla obtained a temperature response curve which increases at about 0.4 percent per °C from about 10°C to 40°C. Although we did not repeat this measurement, we found that the ambient temperature variation of several degrees during the daytime made it difficult to obtain reliable data in the wintertime experiments. All

scattering data was therefore obtained at night, when the temperature variation over a period of 4 or 5 hours was usually less than 0.3°C.

In addition to the steady-state temperature response, the instrument exhibits a transient temperature response which is in the opposite direction; that is, a sudden cooling of the room by 5 or 6°C produces a temporary increase in current reading which returns to its new equilibrium value after about 10 minutes. The origin of this effect was not established, beyond the fact that it is not in the head amplifier or Victoreen resistor and is present with both the air-filled and the evacuated coax and with both the air-filled and the decane-filled chamber. It may be caused by a change in contact potential between the inner and outer conductors which charges and discharges the capacitance in the circuit through the leakage resistance as temperature equilibrium is reestablished.

3. Background

The background current of the decane-filled chamber was lower than we expected. VanDilla found a background of 0.2 mv using a 10^{10} ohm resistor, a collecting voltage of 600v, and a sensitive volume of about 1 cc.

scattering data was therefore obtained at night, when the temperature variation over a period of 4 or 5 hours was usually less than 0.5°C.

In addition to the steady-state temperature response, the instrument exhibits a transient temperature response which is in the opposite direction; that is, a sudden cooling of the room by 5 or 6°C produces a temporary increase in current reading which returns to its new equilibrium value after about 10 minutes. The origin of this effect was not established, beyond the fact that it is not in the load resistor or Wheatstone resistor and is present with both the air-filled and the evacuated coax and with both the air-filled and the dessane-filled chamber. It may be caused by a change in contact potential between the inner and outer conductors which charges and discharges the capacitance in the circuit through the leakage resistance as temperature equilibrium is reestablished.

6. Background

The background current of the dessane-filled chamber was lower than we expected. Vandille found a background of 0.2 mv using a 10^{10} ohm resistor, a collecting voltage of 600v, and a sensitive volume of about 1 cc.

We found backgrounds of about 0.4 mv using a 10^{11} ohm resistor, 1200v collecting voltage, and about 2 cc sensitive volume. The decane was obtained from the same source, Mr. E. J. Curtis, and although it may not have been from the same lot, it received the same type of supplementary processing. The improvement in background may be due to the more nearly symmetrical geometry in the spherical portion of the new shell, which probably reduced the field strength in that portion even at twice the applied voltage.

High backgrounds were obtained in the first few attempts at filling the chamber with decane. A number of changes were made in order to insure a clean filling, so that the factors which produced a high background are not known. The Dag No. 194 coating was changed to Aquadag, as previously mentioned. The decane, which in stock solution was stored in a glass, stoppered bottle with a coil of sodium wire in the bottom to remove moisture, was filtered into a clean, acid-washed glass bottle and stoppered, without adding sodium wire. The pipette used to introduce the decane into the shell through the guard-ring section was acid-cleaned. The cleaning process for all glassware and the Teflon insulators was to wash with soap and water; soak in sulfuric

acid and chromic oxide solution; rinse with tap water, then with distilled water, then with 100 percent ethyl alcohol; and heat until thoroughly dry.

With these precautions the background immediately after filling may be as high as 10 or 20 mv (1 or 2 x 10^{-13} amps), but after several hours it falls to 1 or 2 mv and for the next day or two continues to decrease to a final value of about 0.4 mv. This effect may be due to small amounts of water or some other slightly ionized substance which gradually is electrolized. The stability at these high backgrounds remains poor for several hours indicating that in addition there may be charged colloidal particles in suspension which are rapidly pulled to the walls of the chamber and deposited.

4.[illegible]Stability

The overall stability of the entire measuring system is quite good. During the course of the scattering experiments the source, about 3 mc of Co^{60}, was repositioned each evening. The following data were obtained with a source-chamber separation of 20 cm, where failure to duplicate the source position exactly has less effect than at closer distances.

Table II-1

Date	Temp.	Background	Output
4/9/52	24.0°C	0.48 mv	39.5 mv
4/10/52	25.3°C	0.48 mv	39.7 mv
4/14/52	23.8°C	0.34 mv	39.6 mv
4/15/52	24.4°C	0.33 mv	39.2 mv
4/17/52	26.0°C	0.40 mv	39.0 mv

The maximum fluctuations in these output voltages are about ± 0.4 mv as observed on the recorder chart, and the readings are the average over about 10 minutes.

The vibrating-reed electrometer is an extremely stable and reliable instrument. When it is being used frequently, it should be left running continuously. There is then only a slight drift in the zero setting from day to day, and the drift during the course of an experiment is usually negligible.

There is a slow, continuous decrease of the battery voltage in the Rubicon potentiometer as the batteries age. When the potentiometer is turned off, the batteries, as advertised, tend to regain their voltage. A minimum drift rate is obtained by leaving the potentiometer energized, so that there is a small continuous drain on the batteries. Even so, at large output vol-

Table II-1

Date	Temp.	Background	Output
4/9/52	24.0°C	0.18 mv	89.6 mv
4/10/52	25.8°C	0.17 mv	89.7 mv
4/11/52	25.8°C	0.84 mv	89.6 mv
4/15/52	24.4°C	0.25 mv	89.2 mv
4/17/52	26.0°C	0.10 mv	89.0 mv

The maximum fluctuations in these output voltages are about ± 0.4 mv as observed on the recorder chart, and the readings are the average over about 10 minutes.

The vibrating-reed electrometer is an extremely stable and reliable instrument. When it is being used frequently, it should be left running continuously. There is then only a slight drift in the zero setting from day to day, and the drift during the course of an experiment is usually negligible.

There is a slow, continuous decrease of the battery voltage in the Tudicon potentiometer as the batteries age. When the potentiometer is turned off, the batteries, as advertised, tend to retain their voltage. A minimum drift rate is obtained by leaving the potentiometer energized, so that there is a small continuous drain on the batteries. Even so, at large meter val-

tages the magnitude of the drift may be appreciable over several hours, and it is desirable to balance the battery output against the standard cell at frequent intervals.

There is a slow evaporation of the decane filling which necessitates refilling occasionally. When the shell is filled to the top (with about 3 cc), evaporation to the bottom of the guard ring requires between one and two months. A decrease in sensitivity would result if the level fell below the guard ring, but there is no difficulty in telling when this level is reached. The slightest jarring of the chamber, even the closing of the door to the laboratory, may produce large fluctuations in the output which persist for 5 or 10 minutes. Normally microphonics caused by bumping the chamber or the support of the head amplifier unit are damped out in a few seconds.

The "normal" fluctuations in output voltage were the subject of considerable fruitless investigation. The output voltage varies from about 40 $\pm$ 0.4 mv to 600 $\pm$ 3 mv as the source-chamber separation is changed from about 20 cm to 5 cm. A number of tests were made to see if these fluctuations could be reduced. Two different 10^{11} ohm Victoreen resistors were used, mounted

in two different ways in the head amplifier. While the air-filled coax was being used, the Teflon insulators and the spring contact in the guard-ring section were eliminated by threading the center electrode to the center conductor of the coax. The air-filled coax was replaced by the evacuated coax. Cleaning of the Teflon insulators with soap and water and rinsing with distilled water was replaced by the process previously described. No detectable improvement in "stability" was achieved. At one time an increased instability was observed and was found to be caused by one of the 300v batteries in the battery bank, whose output voltage had dropped to about 240v. All new batteries were installed in the battery bank and in the Rubicon potentiometer, and the fluctuations subsequently remained normal.

Although it is difficult to calculate the statistical fluctuations to be expected, a lower limit can be calculated roughly, using the results of Evans[13] for the statistics of counting rate meters. The fractional standard deviation of a single instantaneous reading of a counting rate meter receiving $\underline{a}$ random pulses per second, each producing a charge, q, is $\sigma(Q)/Q_m = (1/2aRC)^{1/2}$, where RC is the time constant of the circuit

in seconds. When the output is recorded on a chart, about 95 percent of the fluctuations will lie between $\pm 2\sigma$.

In a source of about 3 mc there are about 1.12×10^8 disintegrations per second. There are two γ-rays in cascade from each disintegrating atom of Co^{60}. Although these two γ-rays are not statistically independent, if there is no angular correlation between the two rays and if the solid angle subtended by the chamber is not too large, the γ-rays incident on the chamber can be considered as arriving randomly. Since the probability that an ionizing event will occur is small and random, we should not be far wrong in assuming that the a ionizing events are occurring randomly.

At most the number of ionizing events per second in the chamber is the flux subtended by the solid angle of the chamber times the attenuation of the flux by the chamber. Along the diameter of the chamber there is 1/4" of lucite, density 1.18 g/cc, and 1/2" of decane, density 0.73 g/cc, or a total thickness of 1.67 g/cm^2 of essentially air-equivalent material. At an average energy of 1.25 Mev for the Co^{60} γ-rays the total absorption coefficient in air is about 7.35×10^{-5} cm^{-1} and the mean free path about 17.6 g/cm^2. The detection efficiency is thus about 1.67/17.6 = 0.095. The total cross section

of the chamber containing the sensitive volume is about 3.8 cm^2. The time constant of the circuit was estimated by noting the length of time required for a high voltage reading to reach background when the source was quickly removed. This time was between 5 and 10 seconds and the time constant is then roughly 1.6 seconds ($RC_c = 10^{11} \times 10 \times 10^{-12} = 1$ second). Comparing the calculated and observed values of fractional standard deviation at 20 cm and at 5 cm:

At 20 cm	At 5 cm
$a = 2.24 \times 10^8 \times \frac{3.8}{5020} \times 0.095$	$a = 2.24 \times 10^8 \times \frac{3.8}{3.4} \times 0.095$
$a = 1.6 \times 10^4$	$a = 2.57 \times 10^5$
$2aRC = 5.1 \times 10^4$	$2aRC = 8.2 \times 10^5$
$\sigma_{(Q)}/Q_m = 0.0045$	$\sigma_{(Q)}/Q_m = 0.0011$
$\sigma_{(V)}/V_m = \frac{0.2}{40} = 0.0050$	$\sigma_{(V)}/V_m = \frac{1.5}{600} = 0.0025$

The air-filled chamber gave 20 $\pm$ 0.2 mv output at the 5-cm position. The detection efficiency is reduced to about 0.040 and $\sigma_{(Q)}/Q_m = 0.0017$ as compared with 0.005 from the data.

These calculations give only a rough idea of the order of magnitude of the true statistical fluctuations.

of the chamber containing the sensitive volume is about 5.8 cm^3. The time constant of the circuit was estimated by noting the length of time required for a drop voltage resulting to reach $\frac{1}{e}$ of the normal when the source was shielded removed. This time was between 3 and 10 seconds and the time constant is then roughly 1.5 seconds ($RC = 10^6 \times 10^{-12} = 10 \times 10^{-12} = 1$ second). Comparing the calculated and observed values of fractional standard deviation at 20 cm and at 5 cm:

At 20 cm	At 5 cm
$\epsilon = 2.74 \times 10^4 \times \frac{6.6}{2000} = 0.393$	$\epsilon = 2.74 \times 10^4 \times \frac{6.6}{5.8} = 0.0956$
$n = 1.8 \times 10^4$	$n = 2.87 \times 10^2$
$2\epsilon RC = 8.1 \times 10^4$	$2\epsilon RC = 8.1 \times 10^2$
$\sigma_{(\delta)}/\sigma^m = 0.0440$	$\sigma_{(\delta)}/\sigma^m = 0.0011$
$\sigma_{(A)}/A^m = \frac{20}{6.6} = 0.3030$	$\sigma_{(A)}/A^m = \frac{5.8}{2000} = 0.0029$

The air-filled chamber gave 20 ± 0.1 mv output at the 6-cm position. The detection efficiency is reduced to about 0.040 and $\sigma_{(\delta)}/\sigma^m = 0.0017$ as compared with 0.003 from the data.

These calculations give only a rough idea of the order of magnitude of the true statistical fluctuations.

The geometrical calculations are rough, and the efficiency calculations are too high, because the average thickness of the chamber is less than the full diameter and because the ionizing electrons are predominantly in the forward direction, so that the contributions from the rear wall are probably small. An assumption in this statistical analysis of counting rate meters is that each ionizing event produces the same charge, q. This is not fulfilled in Compton scattering, where the electrons have initial energies from zero to about 1.1 Mev from the γ-rays of Co^{60}. The variations in specific ionization and path length in the chamber tend to make the observed fluctuations greater than the calculated value, and the observed fluctuations are not unreasonably larger than what would be expected simply from the statistical nature of the processes.

The Johnson noise from the resistor R is $\sqrt{4RkT\Delta F}$, where Δf is of the order of magnitude of 10 c.p.s. At $300^{\circ}K$ this amounts to 0.04 mv when $R = 10^{11}$ ohms. The observed fluctuations with the chamber and coax disconnected were about $\pm$ 0.015 mv.

The geometrical calculations are rough, and the efficiency calculations are too high, because the average thickness of the chamber is less than the full diameter and because the ionizing electrons are predominantly in the forward direction, so that the contributions from the rear wall are probably small. An assumption in this calculation analysis of counting rate meters is that each ionizing event produces the same charge,q. This is not fulfilled in Compton scattering, where the electrons have initial energies from zero to about 1.1 Mev from the γ-rays of Co^{60}. The variations in superficial ionization and path length in the chamber tend to make the observed fluctuations greater than the calculated value, and the observed fluctuations are not unreasonably larger than would be expected simply from the statistical nature of the processes.

The johnson noise from the resistor R is $\sqrt{4kTR\Delta f}$, where Δf is of the order of magnitude of 10 c.p.s. At 300°K this amounts to 0.01 ev when R = 10^{11} ohms. The observed fluctuations with the chamber and case disconnected were about ± 0.01a ev.

5. Inverse-square response

The inverse-square response was obtained using the Co^{60} source mounted in a small lucite tube 5 mm in diameter. The source is about 5 mm long and 1 mm in diameter. The results are plotted in Fig. 3. When the air-filled coax was used, it was necessary to average the readings obtained with opposite polarities of the collecting voltage. The collection of ions due to contact potential gives currents which are always in the same direction and cancel out in the average reading. With the evacuated coax installed there is practically no contribution to ion current except in the chamber, and both positive and negative collecting voltages give a flat inverse-square response except at small distances.

The effect of increasing the collecting voltage from 300v to 1200v is a definite improvement in the inverse-square response at small distances and indicates the importance of general recombination. The dosage rate at the chamber with the Co^{60} source at 5 cm is about 1.6 r/hr. VanDilla found that with a 600v collecting voltage the general recombination loss was only about 1 percent at 3.6 r/hr, and this figure is in good agreement with his calculations from the diffusion equation in

6. Inverse-square response

The inverse-square response was obtained using the Co^{60} source mounted in a small lucite tube 3 cm in diameter. The source is about 3 cm long and 1 cm in diameter. The results are plotted in Fig. 6. Even the air-filled cork was used, it was necessary to average the readings obtained with opposite polarities of the collecting voltage. The collection of ions due to contact potential gives currents which are always in the same direction and cancel out in the average reading. With the evacuated cork installed there is practically no contribution to ion current except in the chamber, and both positive and negative collecting voltages give a flat inverse-square response except at small distances.

The effect of increasing the collecting voltage from 300v to 1200v is a definite improvement in the inverse-square response at small distances and indicates the importance of general recombination. The dosage rate at the chamber with the Co^{60} source at 3 cm is about 1.6 r/hr. Ventille found that with a 600v collecting voltage the general recombination loss was only about 1 percent at 1.6 r/hr, and this figure is in good agreement with his calculations from the diffusion equation in

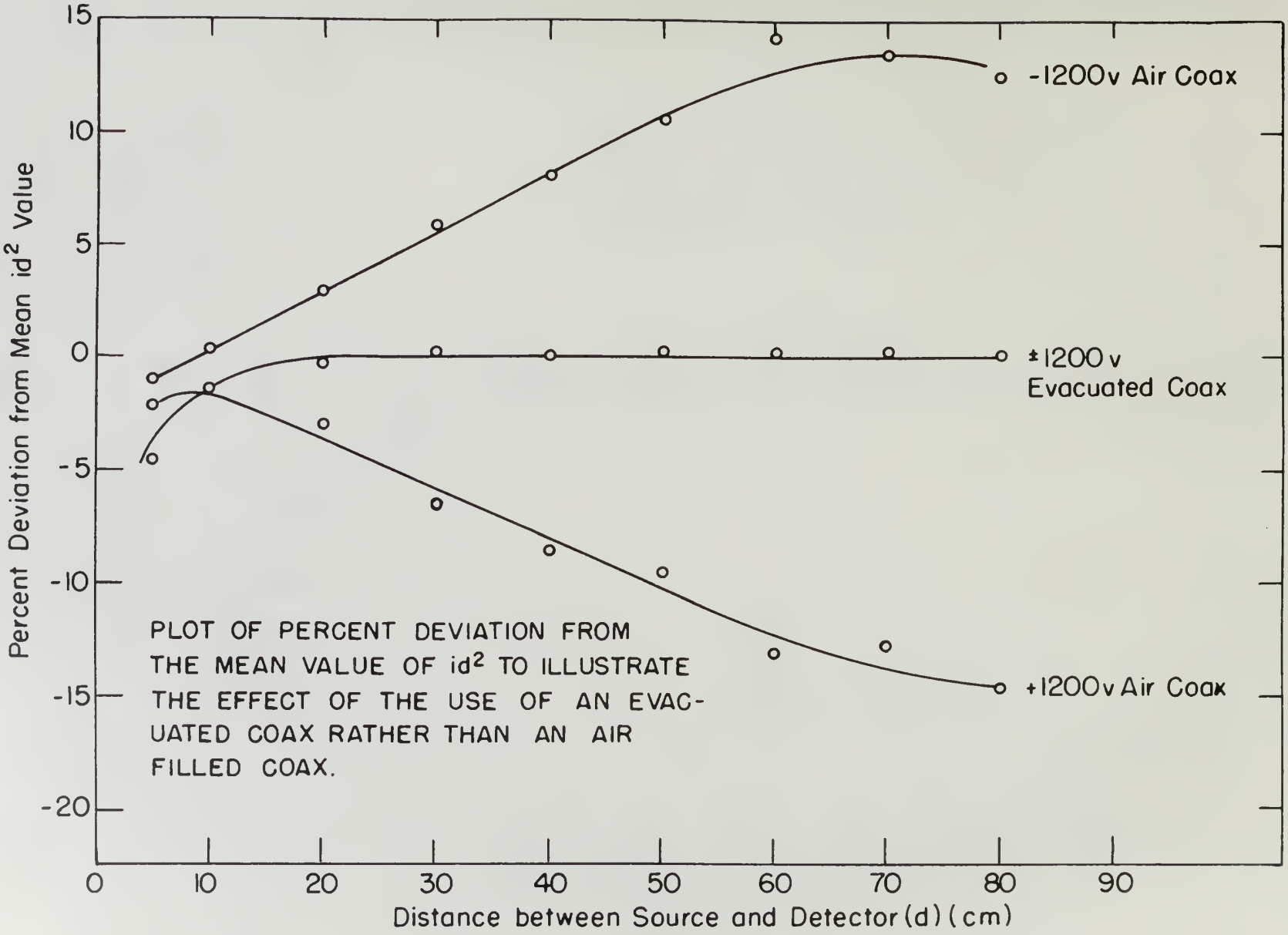
15
10
5
0
-5
-10
-15
-20
Percent Deviation from Mean id² Value
-1200v Air Coax
±1200v
Evacuated Coax
+1200v Air Coax
PLOT OF PERCENT DEVIATION FROM THE MEAN VALUE OF id² TO ILLUSTRATE THE EFFECT OF THE USE OF AN EVACUATED COAX RATHER THAN AN AIR FILLED COAX.
0
10
20
30
40
50
60
70
80
90
Distance between Source and Detector (d) (cm)

Figure 3a

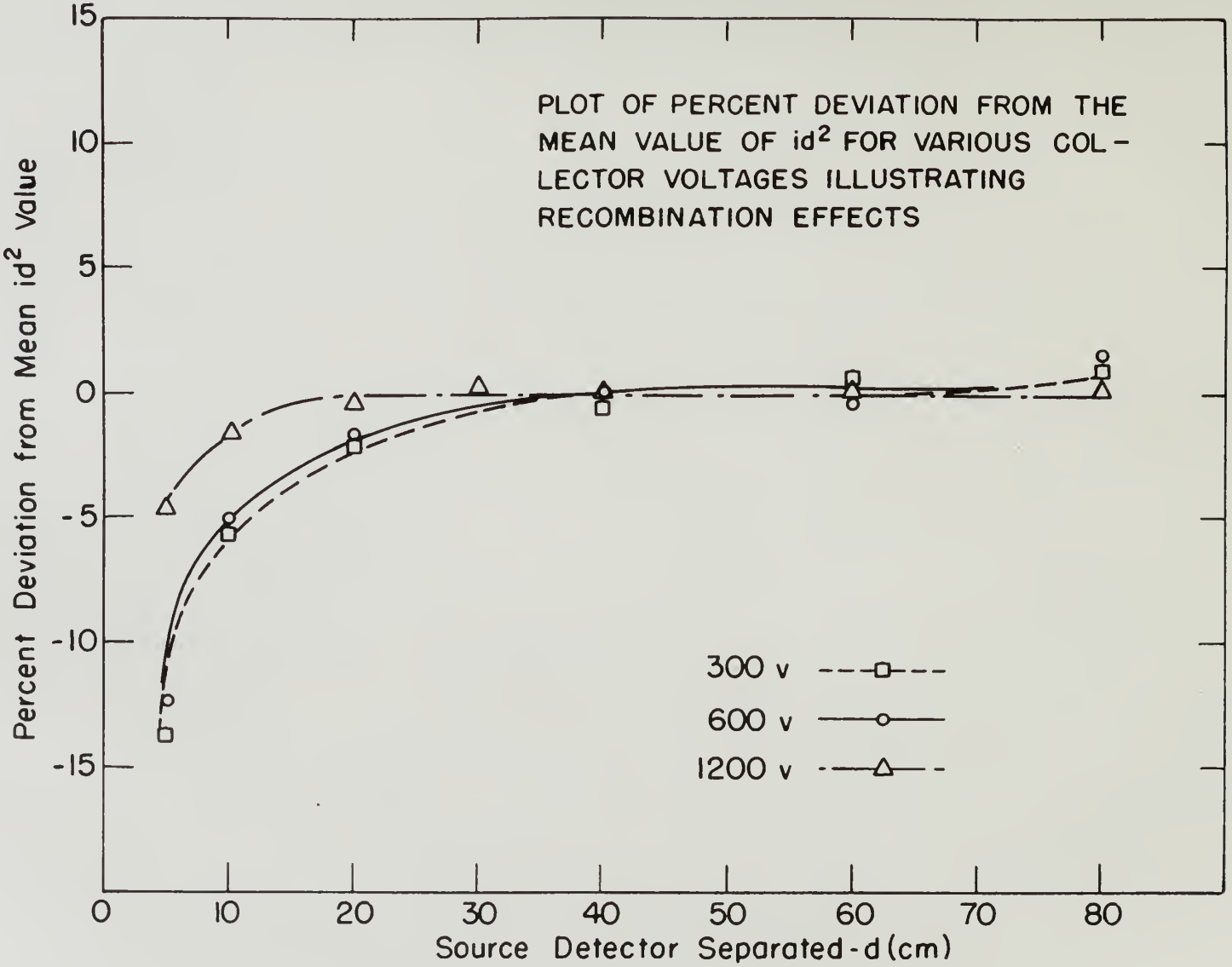
PLOT OF PERCENT DEVIATION FROM THE MEAN VALUE OF id² FOR VARIOUS COL-LECTOR VOLTAGES ILLUSTRATING RECOMBINATION EFFECTS
Percent Deviation from Mean id² Value
15
10
5
0
-5
-10
-15
0
10
20
30
40
50
60
70
80
Source Detector Separated - d (cm)
300 v
600 v
1200 v

Figure 3b

plane geometry. On this basis the general recombination loss at 1200v should be about 1/16 that for 300v at the same dosage rate. Assuming that the departure from ideal inverse-square response is due entirely to general recombination, the fall-off at 5 cm and 1200v should be only about 0.8 percent from the inverse-square data, whereas the actual value is about 4.4 percent.

Part of this departure from ideal inverse-square law response is probably geometrical. Kaye and Binks,[5] using a 2 cc and a 40 cc cylindrical, graphite-wall air chamber, found that the large chamber gave readings which increased too rapidly at small distances, while the small chamber gave a small rise and then a rapid fall-off below about 5 cm. The explanation is that there are two opposing effects: 1) the effective center of the chamber is closer to the source than the geometrical center and 2) the ends of the chamber are further from the source than is the geometrical center. Which of these effects predominates at a given distance depends on the chamber and source geometry. At large distances the source and chamber are effectively points, but scattered radiation and air absorption may have appreciable effect. These, too, are opposing effects, and the net effect in our experiment is apparently negligible.

plane geometry. On this basis the general recombination loss at 1200v should be about 1/16 that for 800v at the same dosage rate. Assuming that the departure from ideal inverse-square response is due entirely to general recombination, the fall-off at 3 cm and 1200v should be only about 0.6 percent from the inverse-square data, whereas the actual value is about 4.4 percent.

Part of this departure from ideal inverse-square law response is probably geometrical. Kaye and Hinks,(5) using a 2 cc and a 40 cc cylindrical, graphite-wall air chamber, found that the large chamber gave readings which increased too rapidly at small distances, while the small chamber gave a small rise and then a rapid fall-off below about 5 cm. The explanation is that there are two opposing effects: 1) the effective center of the chamber is closer to the source than the geometrical center and 2) the ends of the chamber are further from the source than is the geometrical center. Which of these effects predominates at a given distance depends on the chamber and source geometry. At large distances the source and chamber are effectively points, but scattered radiation and air absorption may have appreciable effect. These, too, are opposing effects, and the net effect in our experiment is apparently negligible.

III. PENETRATION OF γ-RAYS THROUGH A MEDIUM

A. γ-Ray Interactions

The problem of the penetration of γ-rays through a large mass of matter is extremely difficult to handle theoretically due to the complex nature of the analytical expressions for the interactions and the fact that multiple interactions will necessarily occur. In the studies being undertaken here, however, the use of medium energy radiation and, in general, light (low Z) materials, results in a situation such that only Compton interactions are of importance. The only exception is found in the investigations involving scattering from lead where photo-absorption becomes an important factor.

The Compton effect alone, however, requires sufficiently complicated equations to describe the interaction to make theoretical treatments extremely difficult. When a photon of energy $h\nu_o$ makes elastic collision with an electron, the electron obtains a fraction of this energy, and the remaining energy appears as a photon of lesser energy $h\nu_1$. In the collision energy and momentum must be conserved, consequently the energy transmitted to the electron and that retained by the photon must

III. PENETRATION OF γ-RAY THROUGH A MEDIUM

A. γ-Ray Interactions

The problem of the penetration of γ-rays through a large mass of matter is extremely difficult to handle theoretically due to the complex nature of the analytical expressions for the interactions and the fact that multiple interactions will necessarily occur. In the studies being undertaken here, however, the use of medium energy radiation and, in general, light (low Z) materials, results in a situation such that only Compton interactions are of importance. The only exception is found in the investigations involving scattering from lead where photo-absorption becomes an important factor.

The Compton effect alone, however, requires sufficiently complicated equations to describe the interaction to make theoretical treatments extremely difficult. When a photon of energy $h\nu_0$ makes elastic collision with an electron, the electron obtains a fraction of this energy, and the remaining energy appears as a photon of lesser energy $h\nu'$. In the collision energy and momentum must be conserved, consequently the energy transmitted to the electron and that retained by the photon must

be such that:

$$\frac{h\nu_1}{h\nu_o} = \frac{1}{1 + a_o(1 - \cos\theta)} \qquad \text{(III-1)}$$

and $$E_r = h\nu_o - h\nu_1$$

for any given scattering angle, θ. Here a_o is the incident photon energy $h\nu_o$ expressed in terms of the rest mass of the electron and E_r is the energy of the recoil electron. These equations are valid for any selected angle θ, but say nothing about the relative probability of scattering at any particular angle. The theory of Klein and Nishina, however, gives the probability per electron for scattering at a given angle per unit solid angle in a single collision as a function of both scattering angle and incident photon energy $h\nu_o$:

$$\frac{d({}_e\sigma)}{d\Omega} = \frac{r_o^2}{2}\left(\frac{\nu_1}{\nu_o}\right)^2\left(\frac{\nu_o}{\nu_1} + \frac{\nu_1}{\nu_o} - \sin^2\theta\right)$$

where r_o is the classical electron radius $e^2/m_o c^2$, ν_1/ν_o is given by Eq. (III-1), and $d\Omega = 2\pi \sin\theta\, d\theta$. The fact that the scattering is such a complex function of the angle θ, along with the change in wavelength with scattering constitute the major source of the mathematical difficulties in a theoretical treatment of the

be such that:

$$\frac{p_{\gamma}^{0}}{h\gamma^{1}} = \frac{1 + \varepsilon^{0}(1 - \cos\theta)}{\varepsilon} \tag{III-f}$$

and $$E^{x} = h\gamma^{0} - h\gamma^{1}$$

for any given scattering angle, θ. Here ε^{0} is the incident photon energy $h\gamma^{0}$ expressed in terms of the rest mass of the electron and E^{x} is the energy of the recoil electron. These equations are valid for any selected angle θ, but say nothing about the relative probability of scattering at any particular angle. The theory of Klein and Nishina, however, gives the probability per electron for scattering at a given angle per unit solid angle in a single collision as a function of both scattering angle and incident photon energy $h\gamma^{0}$:

$$\frac{dU}{d(\cos\theta)} = \frac{\pi}{2}\left(\frac{e^{2}}{mc^{2}}\right)^{2}\left(\frac{\lambda^{1}}{\lambda^{0}} + \frac{\lambda^{0}}{\lambda^{1}} - \sin^{2}\theta\right)$$

where r^{0} is the classical electron radius e^{2}/mc^{2}, λ^{1}/λ^{0} is given by Eq. (III-f), and $d\Omega = 2\pi \sin\theta\, d\theta$. The fact that the scattering is such a complex function of the angle θ, along with the change in wavelength with scattering constitute the major source of the mathematical difficulties in a theoretical treatment of the

scattering problem. If the incident photons are monoenergetic and make only a single collision it is possible, although tedious, to use the preceding equations to calculate the energy and angular distribution of the continuous spectrum of degraded photons resulting therefrom. When, however, multiple collisions are considered, with successive energy degradations, the mathematical difficulties become extreme, so that only approximate theories are available to date. In fact, this last statement also applies to neutron collisions which are much less complex in nature.(14)

Compton scattering is strongly anisotropic. At large quantum energies most of the scattering tends to occur in the forward direction in a small angled cone about the direction of the incident photons. From the Klein-Nishina equation, Davisson(15) has calculated the fraction of the singly scattered photon energy which is scattered between 0° and θ up to $\theta = 180^{\circ}$ for various incident energies a_0. From these calculations the angle $\theta_{1/2}$ containing half the scattered energy flux can be calculated. This is presented in Table III-1, on the following page. From this table it is obvious that the cone containing half the scattered energy opens slowly as the incident photon energy decreases until it

approaches 90° at small a_o.

Table III-1

$h\nu/m_oc^2 \equiv a_o$	10	4	2	1	0.4	0.1	0.0
$\theta_{1/2}$	20°	29°	38°	47°	62°	78°	90°

When considering interactions between medium energy photons and heavy (highZ) materials the photoelectric effect also becomes important. Either the primary photons, the Compton-scattered photons, or both may be completely absorbed by an atom, resulting in the ejection of an atomic electron having the full photon energy less its own binding energy. This interaction acts as a sink for photons in the medium preventing their excape from or further scattering within the medium. This effect is of importance, however, only for low quantum energies in light materials, or for medium ($\sim$ 1 Mev) energies in heavy material.

B. Review of Previous Studies of γ-Ray Penetration

Considerable theoretical and experimental work has been done on the penetration of photons through absorbers. We are here most interested in studies where a

approximate 90° at small θ°.

Table III-I

$h\nu/m_0c^2 \equiv \alpha^{-1}$	$\theta_1/2$	θ_0	θ_{90}	θ_{45}	θ_{30}	θ_{20}	θ_{10}	θ_5
10	$\frac{1}{4}$	-	1	0.4	0.1	0.4		

When competing interactions between medium energy photons and heavy (atom) materials the photoelectric effect also becomes important. Either the primary photons, the Compton-scattered photons, or both may be completely absorbed by an atom, resulting in the ejection of an atomic electron having the full photon energy less its own binding energy. This interaction acts as a sink for photons in the medium preventing their escape from or further scattering within the medium. This effect is of importance, however, only for low energies in light materials, or for medium ($\sim$ 1 Mev) energies in heavy material.

5. Review of Previous Studies of γ-Ray Penetration

Considerable theoretical and experimental work has been done on the penetration of gamma rays. It is here most interested in studies which

small radioactive source is embedded inside a thick absorber along with an imbedded detector in an attempt to determine if studies utilizing a semi-infinite medium can be utilized to predict behavior in an infinite (very thick) medium.

1. Gray[3] in a series of measurements using a large aluminum cylinder (40 cm in diameter and 60 cm long) with the source and detector imbedded in a central hole and separated by aluminum plugs found that scattering never compensated for absorption. Values of the build-up factor in aluminum have been calculated from Gray's results for comparison with the results obtained when using a semi-infinite mass. This is discussed in Section IV-C below.

2. Lamerton[16] has made extensive calculations on the penetration of X-ray beams of energy up to 2.6 Mev through tissue-like media. He sets up the integral describing the effects of single scattering and evaluates it both numerically and analytically (by using a simpler approximation to the Klein-Nishina formulation). He calculates the effects of multiple scattering, approximately, using the assumption that an equilibrium is set up with respect to scattered radiation of orders higher than the first. This gives an approximation of

the total dosage and the percent due to scattered radiation. The results, however, are rough and applicable only on the axis of a beam.

3. In an attempt to solve the beam penetration problem theoretically, Hirschfelder et al[17,18] developed a method for estimating the intensity of γ-rays which have passed through a thick absorber. While the theory is only approximate it is worthy of study since it is of considerable assistance in obtaining a physical feeling for the problem of multiple scattering without getting too greatly involved in mathematical detail.

(a) Their approach considers the case of a broad beam of monochromatic γ-rays of energy $h\nu_o$ incident normally on a thick absorber (made up of light material so that Compton scattering predominates). They then break up the radiation at any depth in the absorber into unscattered, singly, doubly, etc. scattered photons and attempt to calculate the X-component of each of these groups. This, of course, can be done exactly in the case of singly scattered photons by setting up the integral describing the amount of radiation scattered by a volume element to a point beyond the absorber (as has been done in Reference 19). The mathematics is simplified since the only variable of inte-

gration is the scattering angle ϕ. The integral is, however, still difficult to handle analytically due to the complicated form of the Klein-Nishina formula. Consequently the authors integrate it numerically and tabulate the intensity of the singly-scattered photons for various initial energies $h\nu_o$ and slab thicknesses X. The results are then interpreted in terms of an average angle of scattering $\bar{\phi}$ chosen such that the same emergent intensity (X-component) would result if all the photons were deflected through $\bar{\phi}$ rather than over the distribution of angles which actually obtains. Values of $\bar{\phi}$ are calculated for various $h\nu$ and slab thicknesses to be utilized in multiple-scattering calculations. All singly-scattered photons are assumed to be scattered at the same angle $\bar{\phi}_o$, determined by $h\nu_o$. This fixes their energy $h\nu_1$. But the average scattering angle of photons of energy $h\nu_1$ has already been calculated so that $\bar{\phi}_1$, the average angle of deflection of the doubly-scattered photons, is known. This then fixes their quantum energy $h\nu_2$. Thus the i^{th}-scattered photons are considered as all having the same angle of deflection and energy. This substitution for the actual continuous spectrum simplifies the mathematics considerably. Hirschfelder et al then set up a differential equation for the i^{th} beam,

stating that the change in the X-component of the i^{th}-scattered photons in layer dX is the difference between the increase due to the (i-1)th-scattered photons which undergo one more scattering in dX and the loss due to the scattering in dX of those photons which have already undergone i scatterings. Each beam is thus given by the solution of a differential equation of this type which is very closely analogous to the differential equations for series radioactive decay. The sum of these solutions then gives the X-component of the energy intensity emergent from the slab. The dose is then taken to be proportional to the gradient of this energy intensity.

(b) From this they present tables of values of the X-component of the intensity and average quantum energy of the unscattered, singly, doubly, etc. scattered photons (up to i = 5) emergent from slabs of various thicknesses. (These values are exact, however, only for the unscattered and singly-scattered photons.) Using curve fitting methods they then obtain analytical expressions for both emergent total intensity and dose. For example, for $a = h\nu_o/m_o c^2 = 2$,

$$\frac{I_t}{I_{inc}} = \frac{\text{total emergent intensity (X-component)}}{\text{incident intensity}} \qquad \text{(III-2)}$$

$$\frac{I_t}{I_{inc}} = (1 + 0.487D + 0.030D^2)e^{-D} \qquad \text{(III-3)}$$

$$\text{dose} \propto -\frac{d}{dD}\left(\frac{I_t}{I_{inc}}\right) = \frac{I_t}{I_{inc}} - (0.527 + 0.073D^2)e^{-3D/2} \qquad \text{(III-4)}$$

and for a = 10

$$\frac{I_t}{I_{inc}} = (1 + 0.33D + 0.004D^2)e^{-D} \qquad \text{(III-5)}$$

$$-\frac{d}{dD}\left(\frac{I_t}{I_{inc}}\right) = \frac{I_t}{I_{inc}} - (0.38 + 0.01D + 0.02D^2)e^{-3D/2} \qquad \text{(III-6)}$$

where D is the slab thickness in mean free paths of the incident photons and I_{inc} is the incident intensity. In Eqs. (III-4) and (III-5) the coefficient of e^{-D} is essentially the build-up factor expressing the ratio of total to primary radiation as a function of depth of penetration. This ratio obviously increases faster than linearly with D and does not approach a limiting value for large D. The equation differs from the intensity equations in their dependence on D through the $e^{-3D/2}$ term.

$$\frac{I^t}{I^t_{inc}} = \frac{\text{total scattered intensity (i-component)}}{\text{incident intensity}} \qquad \text{(III-3)}$$

$$\frac{I^t}{I^t_{inc}} = (1 + 0.\text{A}\sigma^2 + 0.0\sigma^2)e^{-D} \qquad \text{(III-4)}$$

$$\text{Some } \epsilon = \frac{\partial D}{\partial}\left(\frac{I^t}{I^t_{inc}}\right) + \frac{I^t}{I^t_{inc}} = (0.\sigma + 0.\text{mc}^2)e^{-D\sigma^2} \qquad \text{(III-4)}$$

and for $\epsilon = 10$

$$\frac{I^t}{I^t_{inc}} = (1 + 0.\sigma + 0.\sigma\text{k}^2)e^{-D} \qquad \text{(III-5)}$$

$$-\frac{\partial D}{\partial}\left(\frac{I^t}{I^t_{inc}}\right) + \frac{I^t}{I^t_{inc}} = (3.\sigma + \ldots + 0.\sigma^2)e^{-D\sigma^2} \qquad \text{(III-6)}$$

where D is the slab thickness in mean free paths of the incident photons and I^{inc} is the incident intensity. In Eqs. (III-1) and (III-6) the coefficient of e^{-D} is essentially the multi-up factor accounting the ratio of total to primary radiation as a function of depth of penetration. This ratio obviously increases faster than linearly with D and does not approach a limiting value for large D. The equation differs from the intensity equations in their dependence on D through the $e^{-\sigma D^2}$ term.

This is appreciable only at small D and represents the fact that the Compton absorption coefficient σ_a is energy dependent.

(c) Hirschfelder also tabulates information concerning the spectrum of the scattered radiation which gives further information on the penetration problem. From a data presented the exponential attenuation of the primaries and the build-up and attenuation of the scattered beams in a manner that resembles series radioactive decay may be readily seen. It also shows that the total transmitted beam has a greater intensity than the primary beam, with the ratio increasing with D.

4. Fano and others[20,21,22,23] have developed theoretical methods for calculation of the radiation field of a point source of γ-rays in an infinite absorbing medium, and have also carried out experiments, the results of which appear to support the theory. The express experimental results in terms of a "build-up factor" defined as the ratio of observed total dosage rate to the dosage rate expected on a basis of good geometry absorption only.

$$\text{BF} = \text{build-up factor} \equiv \frac{\text{observed dosage rate}}{\text{primary dosage rate}}$$

$$= 1 + \frac{\text{dosage rate due to scattered radiation}}{\text{primary dosage rate}}$$

If one considered that an equilibrium were reached between the primary and secondary radiation this quantity would be expected to asymptotically approach a constant value greater than unity at large distances from the source. This concept of equilibrium implies that the ratio of secondary radiation to primary approaches, asymptotically, a constant value, and that the quality of the radiation becomes independent of the depth of penetration. This is, however, not the case. Some of the scattered photons are only infinitesimally softer than the primaries and are deflected through only infinitesimal angles. As a result the assumed approach to equilibrium is prevented. Fano et al predict a build-up factor αr^k, where k is a constant of the order of unity which depends on h and the absorber, and where $r >> 1$ mfp. In addition Spencer and Fano[24] report another approach complementary to that of the earlier papers. Calculations of the build-up factor of Co^{60} in water are in good agreement with the experimental results obtained by White.[1]

5. Foldy and Osborn[25] have developed a theory mainly applicable to light absorbers and photon energies such that the total absorption coefficient is approximately constant. They obtain an approximate solution

to the diffusion equation describing the change in the number of photons having energies and angles in a given range in going through an infinitesimal thickness at any depth. They limit themselves, however, to high-energy photons by their use of the small angle approximation. This results in a fairly simple analytical expression for the spectral distribution of the radiation at any depth X, which, when applied to Co^{60} γ-rays predicts a spectrum of the general shape of that obtained by Spencer and Fano, but with too large a soft component (due to approximations used in the solution).

6. R. D. Evans (unpublished) suggests a simple semi-empirical treatment of a point source in a homogeneous medium, making use of the fact that the ratio of secondary dose rate to primary dose rate is approximately proportional to the distance from the source. He considers a point source of γ-rays in an infinite medium emitting N photons per second of energy E. Let dR be the energy absorption per second in a spherical shell, about the source, of radius r and thickness dr. Then the total energy absorption rate from the primaries is

$$\int_{r=0}^{\infty} dR_{prim} = NE \frac{\mu_a}{\mu_o}$$

where $\mu_a = \tau + \kappa + \sigma_a$

and $\mu_o = \tau + \kappa + \sigma_a + \sigma_s$

Since μ_a/μ_o is the fractional energy lost per primary photon per collision, and each primary photon makes exactly one collision, the total energy absorption rate in the medium is NE, so the scattered radiation delivers a total energy to the medium given by:

$$R_{sec} = NE - NE \frac{\mu_a}{\mu_o} = NE \frac{\sigma_s}{\mu_o}$$

Making use of the experimental fact that the build-up factor BF increases somewhat faster than linearly with r, assume

$$\frac{dR_{sec}}{dR_{prim}} = a(\mu_o r)^k$$

where k is slightly greater than unity, and is a function of photon energy E and the atomic number of the absorbing medium. Integration then gives a value of R_{sec} which can be set equal to that obtained above to obtain a relation between a and k. Thus:

$$\int_{\omega_c}^{\infty} q(\omega)\,d\omega = \frac{k^2}{c^2}$$

where $k^2 = k_x^2 + k_y^2 + \alpha^2$

and $k_0^2 = k_x^2 + k_y^2 + \alpha_0^2$

Since h^2/k^2 is the fractional energy lost per primary photon per collision, and each primary photon makes exactly one collision, the total energy absorption rate in the medium is W, so the scattered radiation delivers a total energy to the medium given by:

$$W^{abs} = W - \pi\frac{r^2}{k^2} = W\frac{\alpha^2}{q^2}$$

Making use of the exponential fact that the multiplying factor by successive scatterings falls linearly with r, assume

$$\frac{dW^{abs}}{dr} = \alpha(\beta_0 r)$$

where β is slightly greater than unity, and is a function of photon energy Σ and the atomic number of the scattering medium. Integration then gives a value of W^{abs} a multiple between α and α_0. Thus:

$$dR_{sec} = a(\mu_o r)^k \left[NE\ e^{-\mu_o r}\ \mu_a\ d_r \right]$$

$$R_{sec} = a\ NE \frac{\mu_a}{\mu_o} \int_o^{\infty} (\mu_o r)^k\ e^{-\mu_o r}\ d(\mu_o r)$$

$$= a\ NE \frac{\mu_o}{\mu_a} \Gamma(K+1) = a\ NE \frac{\mu_o}{\mu_a}\ k\,\Gamma(k)$$

Equating this to $NE \frac{\sigma_s}{\mu_o}$ gives

$$a = \frac{1}{k\,\Gamma(k)} \frac{\sigma_s}{\mu_o}$$

so that the build-up factor is given by

$$BF = 1 + \frac{dR_{sec}}{dR_{prim}} = 1 + \frac{1}{k\,\Gamma(k)} \frac{\sigma_s}{\mu_o} (\mu_o r)^k$$

The unknown k can then be evaluated by calculating BF as a function of $\mu_o r$ for several k, and determining which best fits the true BF.

$$q_{2}^{\text{free}} = \pi(\pi^{0}\tau)_{R}\left[\text{RE} \equiv e^{-\pi^{0}\tau} \pi^{0} e^{\pi^{0}}\right]$$

$$R^{\text{free}} = 2\ \text{RE}\ \frac{\pi^{0}}{\Gamma^{0}} \int_{0}^{\infty} (\pi^{0}\tau)_{R} \equiv^{-\pi^{0}\tau} q(\pi^{0}\tau)$$

$$= \pi\ \text{RE}\ \frac{\pi^{0}}{\pi^{0}}\, L(K+1) = 2\ \text{RE}\ \frac{\pi^{0}}{\pi^{0}}\, \pi\, L(\kappa)$$

Summing this to RE $\frac{\eta^{0}}{\zeta^{0}}$ gives

$$\kappa = \frac{\varepsilon\, L(\varepsilon)}{\Gamma}\, \frac{\pi^{0}}{\zeta^{0}}$$

so that the build-up factor is given by

$$\text{Bf} = 1 + \frac{\text{RE}^{\text{scatt}}}{\text{RE}^{\text{uncol}}} = 1 + \frac{\varepsilon\, L(\varepsilon)}{\Gamma}\, \frac{\pi^{0}}{\zeta^{0}}\, (\pi^{0}\tau)_{R}$$

The unknown ε can then be evaluated by successively if as a function of $\pi^{0}\tau$ for several κ, and determining which best fits the term RE.

IV. EXPERIMENTAL RESULTS

A. Procedure

1. Side scattering

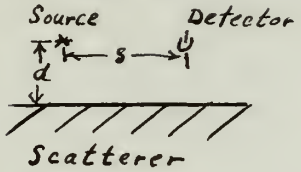

Fig. 4a - Side Scattering

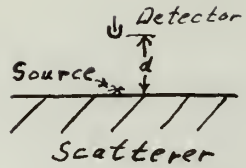

Fig. 4b - Backscattering

Fig. 4 - Diagrams of Experimental Set-ups.

The scattering media investigated were water, aluminum, iron, and lead. To approximate semi-infinite media for source-chamber separations up to 20 cm, the following materials were used:

Water - a glass aquarium filled with water giving a medium 30 cm wide, 30 cm deep, and 50 cm long.

Aluminum - four aluminum blocks giving a medium 33 cm wide, 10 cm deep, and 33 cm long.

Iron - one piece 20 cm wide, 6 cm deep, and 36 cm long.

Lead - three lead bricks giving a medium 30 cm wide, 7.3 cm deep, and 30 cm long.

The Co^{60} source in its small lucite tube was mounted at the end of a plastic rod. One side of the tube

Fig. 3a - Side Scattering

Fig. 3b - Back Scattering

was filed flat so that the 5-mm length of Co^{60} wire could lie horizontally and practically in contact with the scattering medium. In the "side-scattering" experiments the mounting was suspended from a horizontal rod and adjusted to be in contact with the scattering medium when the bottom of the chamber just touched the medium. Approximate source-chamber separations, s, of 5 cm, 10 cm, 15 cm, and 20 cm were used. The actual positions were marked on the horizontal rod and could be duplicated within about 1/4 mm.

The distance d between the source-chamber plane and the surface of the scattering medium was adjusted by placing the medium on a 12" square metal plate welded to the top of a small hydraulic jack, which was used to raise and lower the medium. The distance d could be measured to about $\pm$ 0.1 mm.

2. Back-scattering

For these measurements the source was mounted to lie beneath the chamber and in contact with the scattering medium. Approximately 5 and 10 cm separations between the medium and the bottom of the chamber were used.

was filed flat so that the 3-mm length of Co^{60} wire could lie horizontally and practically in contact with the scattering medium. In the "rid-scattering" experiments the mounting was suspended from a horizontal rod and adjusted to be in contact with the scattering medium when the bottom of the chamber just touched the medium. Appropriate source-chamber separations, s, of 5 cm, 10 cm, 15 cm, and 20 cm were used. The actual positions were marked on the horizontal rod and could be duplicated within about 1/4 mm.

The distance d between the source-chamber plane and the surface of the scattering medium was adjusted by placing the medium on a 1/2" square metal plate welded to the top of a small cylindric jack, which was used to raise and lower the medium. The distance d could be measured to about ± 0.1 mm.

2. Beef-scattering

For these measurements the source was mounted to lie beneath the chamber and in contact with the scattering medium. Approximately 4 and 10 cm separations between the medium and the bottom of the chamber were used.

B. Results

1. Side-scattering

The percentage increase in chamber current due to scattering, as the scattering medium is brought from d = 10 cm to d = 0 cm, is shown in Figs. 5, 6, 7, and 8. The percentage increase is based on the reading obtained with the scattering medium and the jack removed. The scattering from the environment was shown to be quite small from the inverse-square response, so that the scattering from the floor beneath the medium should be negligible. This was borne out by the fact that a 4" thickness of wood larger in area than the media, which was placed on the floor to raise the level of the jack in some of the measurements, made no detectable change in reading when it was removed. The results of VanDilla[2] and Faust[26] indicate that a thickness of about half a mean free path is sufficient to approximate an infinite thickness of medium.

At small separations, s, and small distances, d, the media are good approximations to semi-infinite media. At the extreme position where the separation is 20 cm and the medium is 10 cm below the source and chamber the readings may be somewhat low. The effect of decreasing

5. Results

1. Side-scattering

The percentage increase in counter current due to scattering, as the scattering medium is removed from d = 10 cm to d = 0 cm, is shown in Figs. 3, 4, 7, and 8. The percentage increase is based on the reading obtained with the scattering medium and the lead removed. The scattering from the environment was shown to be quite small from the inverse-square response, so that the scattering from the floor beneath the medium should be negligible. This was borne out by the fact that a 4" thickness of wood lumber in area than the media, which was placed on the floor to raise the level of the lead in zone of the measurements, made no detectable change in reading when it was removed. The results of Metcalf[3] and Grant[26] indicate that a thickness of about half a mean free path is sufficient to approximate an infinite thickness of medium.

At small separations, 3, and small distances, 6, the media are good approximations to semi-infinite media. At the widest position where the separation is 20 cm and the medium is 10 cm below the source and chamber the readings may be somewhat low. The effect of decreasing

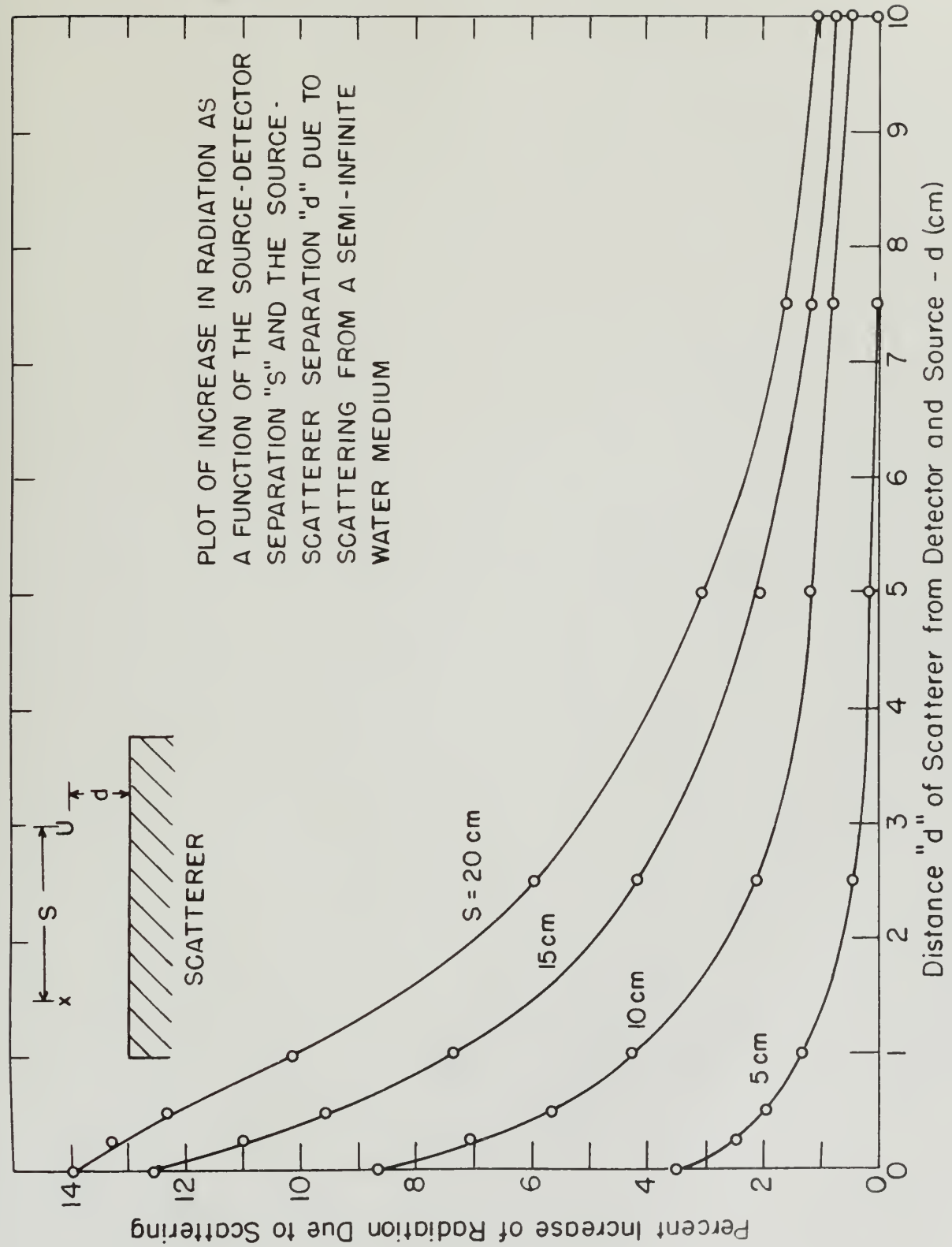
PLOT OF INCREASE IN RADIATION AS
A FUNCTION OF THE SOURCE-DETECTOR
SEPARATION "S" AND THE SOURCE-
SCATTERER SEPARATION "d" DUE TO
SCATTERING FROM A SEMI-INFINITE
WATER MEDIUM
SCATTERER
S
U
d
x
S = 20 cm
15 cm
10 cm
5 cm
Percent Increase of Radiation Due to Scattering
Distance "d" of Scatterer from Detector and Source - d (cm)
0
2
4
6
8
10
12
14
0
1
2
3
4
5
6
7
8
9
10

Figure 5

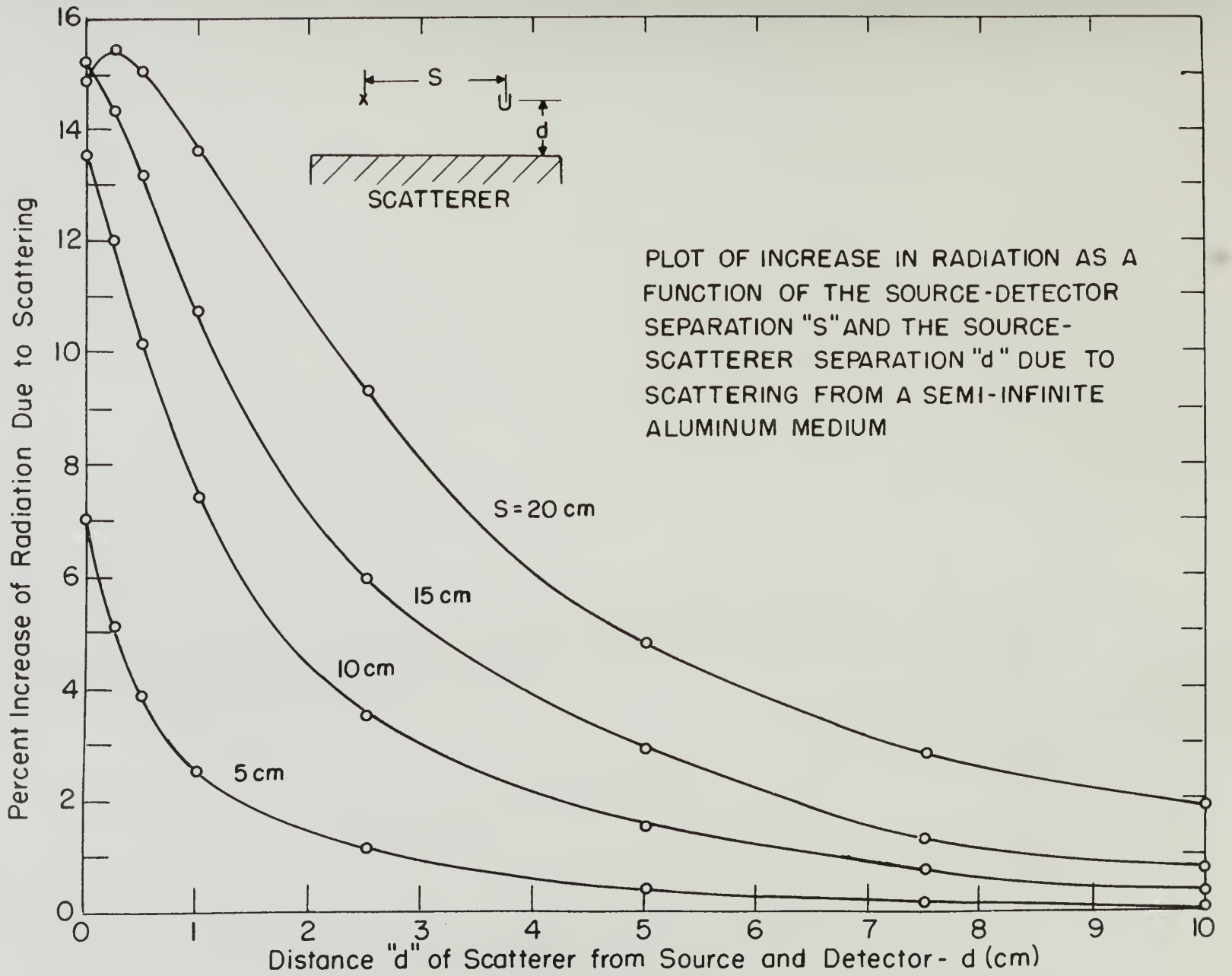
PLOT OF INCREASE IN RADIATION AS A FUNCTION OF THE SOURCE-DETECTOR SEPARATION "S" AND THE SOURCE-SCATTERER SEPARATION "d" DUE TO SCATTERING FROM A SEMI-INFINITE ALUMINUM MEDIUM
S
d
SCATTERER
S=20 cm
15 cm
10 cm
5 cm
Percent Increase of Radiation Due to Scattering
Distance "d" of Scatterer from Source and Detector - d (cm)
0
2
4
6
8
10
12
14
16
0
1
2
3
4
5
6
7
8
9
10

Figure 6

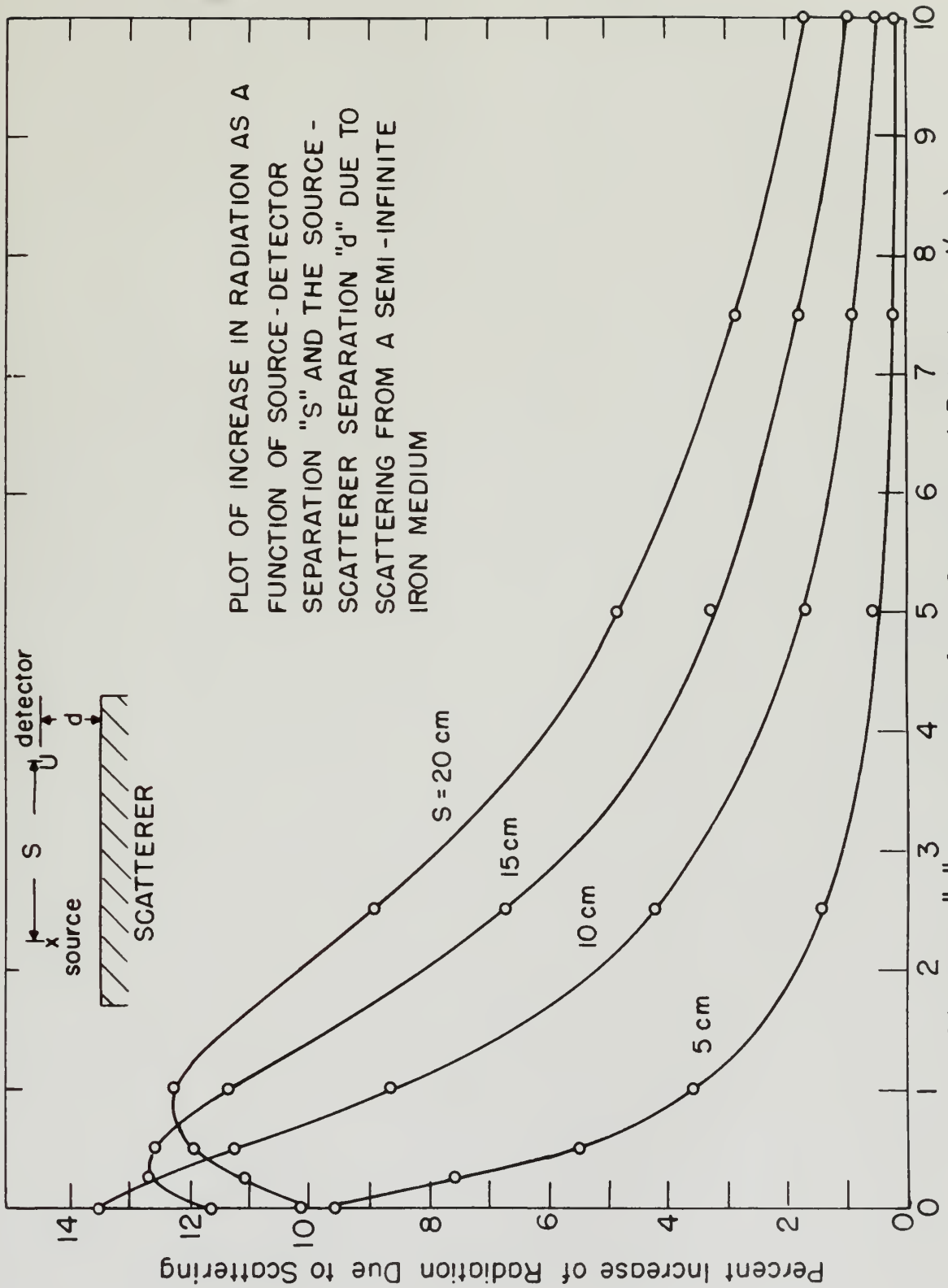
PLOT OF INCREASE IN RADIATION AS A FUNCTION OF SOURCE-DETECTOR SEPARATION "S" AND THE SOURCE-SCATTERER SEPARATION "d" DUE TO SCATTERING FROM A SEMI-INFINITE IRON MEDIUM
source
S
detector
d
SCATTERER
S = 20 cm
15 cm
10 cm
5 cm
Percent Increase of Radiation Due to Scattering
Distance "d" of Scatterer from Source and Detector - d(cm)
0
2
4
6
8
10
12
14
0
1
2
3
4
5
6
7
8
9
10

Figure 7

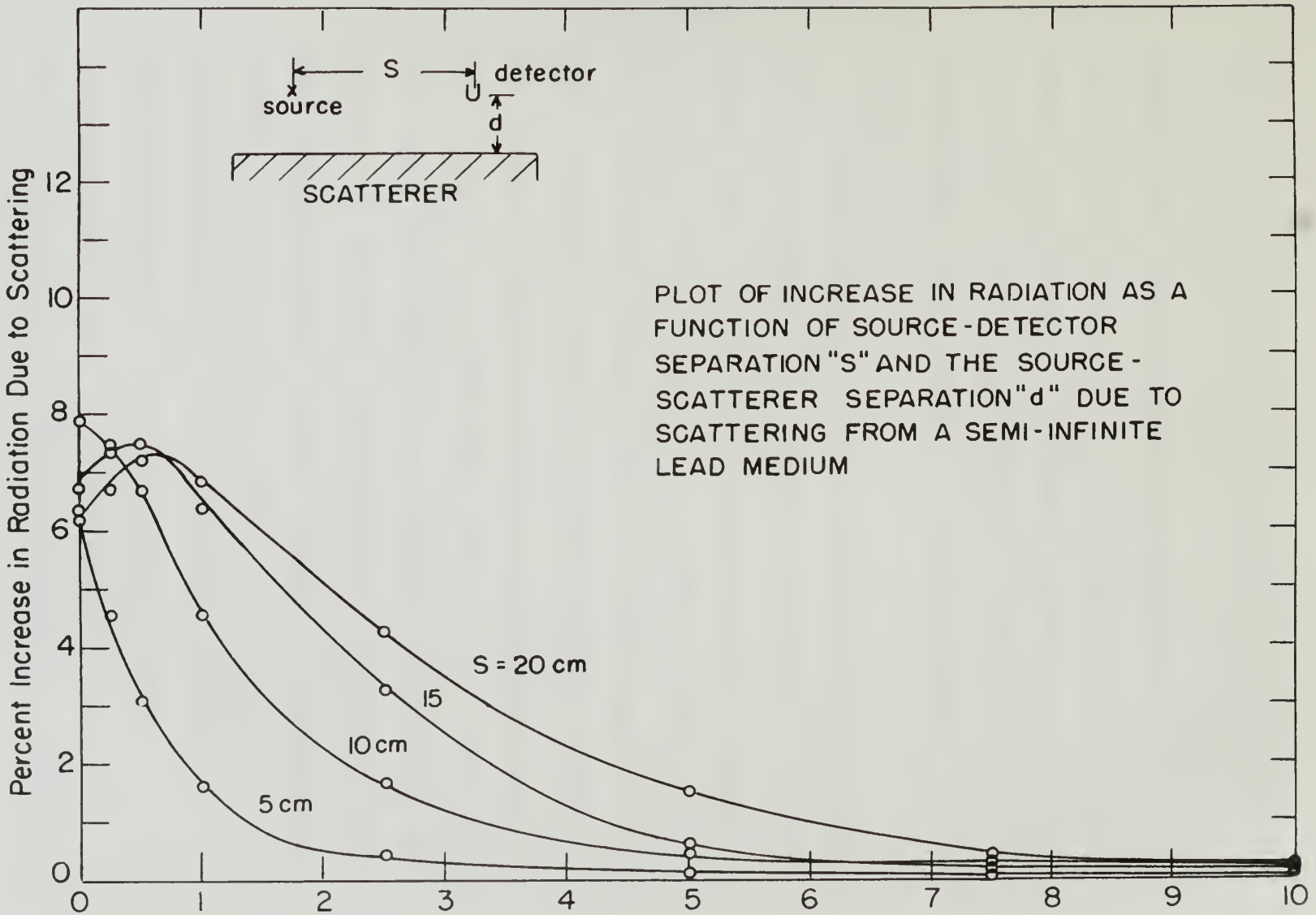
S
detector
source
d
SCATTERER
PLOT OF INCREASE IN RADIATION AS A FUNCTION OF SOURCE-DETECTOR SEPARATION "S" AND THE SOURCE-SCATTERER SEPARATION "d" DUE TO SCATTERING FROM A SEMI-INFINITE LEAD MEDIUM
S = 20 cm
15
10 cm
5 cm
Percent Increase in Radiation Due to Scattering
0
2
4
6
8
10
12
0
1
2
3
4
5
6
7
8
9
10
Distance "d" of Scatterer from Source and Detector - d (cm)
Figure 8

the size and thickness of the medium was observed by using various combinations of the four aluminum blocks for a source-chamber separation of 20 cm. When the distance d is less than 2.5 cm, no detectable difference was observed. When the distance d is 10 cm, the decrease with a half-width of aluminum was about 0.5 percent. The accuracy of the measurement is about ± 0.25 percent.

The measurements at all positions would be expected to be somewhat low, because the response of the chamber falls off at photon energies below 400 kev. How serious this loss will be depends on how much of the total photon energy incident on the chamber is carried by photons in this non-linear response region. The losses in these experiments are probably rather small because at separations which are less than two or three mean free paths of the primary radiation in the medium, the principal contribution to scattered flux is from singly-scattered Compton photons. VanDilla has estimated this loss at 2-3 mfp's in an infinite medium, considering the Co^{60} γ-rays and equal contributions by singly and doubly scattered photons, as about 1 percent. At larger separations in terms of mfp we are using materials whose photoelectric cross-section is becoming

the size and thickness of the media was observed by using various combinations of the four aluminum blocks for a source-chamber separation of 20 cm. When the distance $\underline{d}$ is less than 2.5 cm, no detectable difference was observed. When the distance $\underline{d}$ is 10 cm, the decrease with a half-width of aluminum was about 0.5 percent. The accuracy of the measurement is about $\pm$ 0.25 percent.

The measurements at all positions would be expected to be somewhat low, because the response of the chamber falls off at proton energies below 400 kev. How serious this loss will be depends on how much of the total photon energy incident on the chamber is exerted by photons in this non-linear response region. The losses in these experiments are probably rather small because at exposures which are less than two or three mean free paths of the primary radiation in the medium, the principal contribution to scattered flux is from singly-scattered Compton photons. VenGrila has estimated this loss at 2-3 mr/r in an infinite medium, considering the Co^{60} γ-rays and annual penetrations by singly and doubly scattered photons, as about 1 percent. At larger penetrations in terms of mfp we are using materials whose photoelectric cross-section is becoming

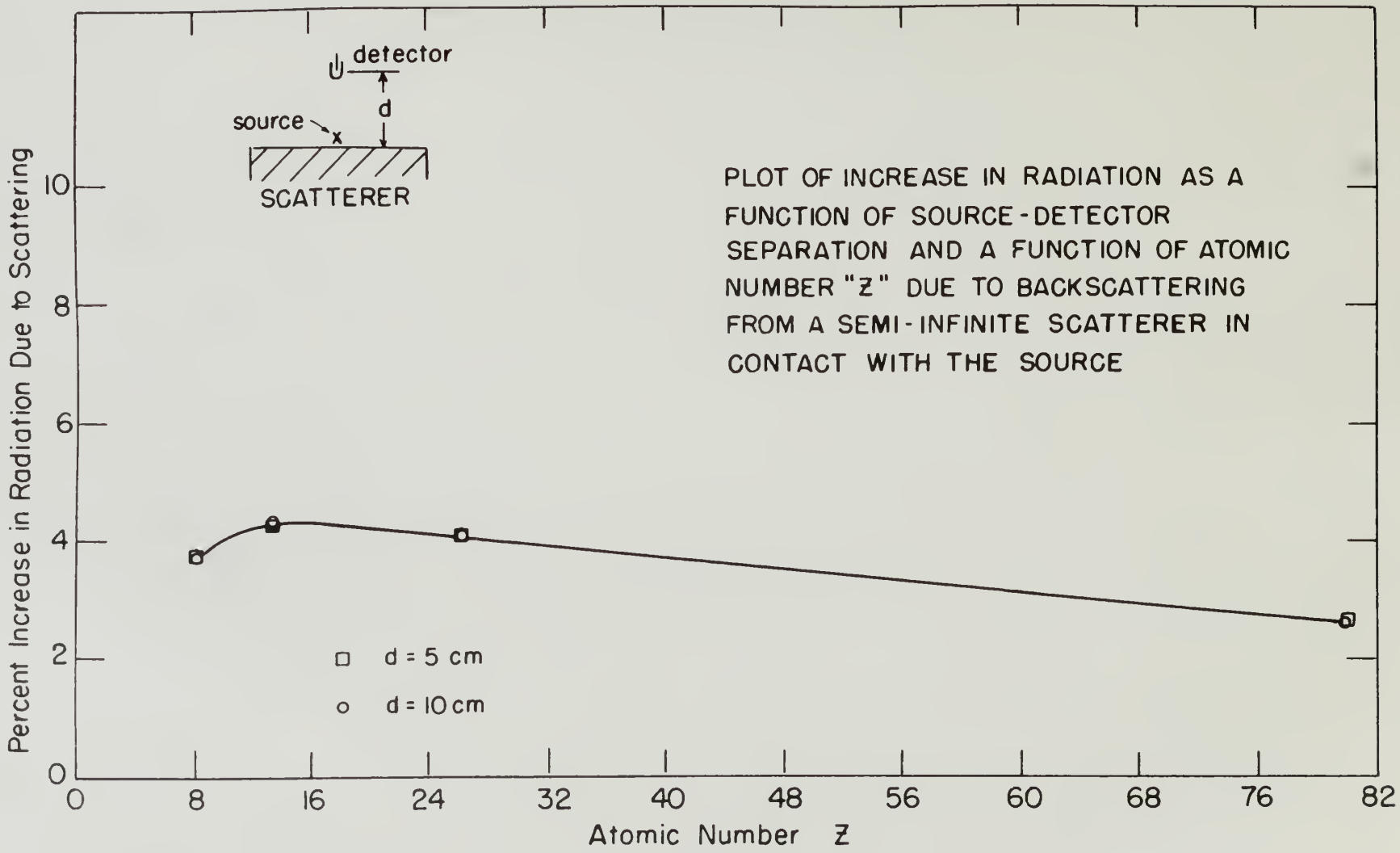
detector
d
source
x
SCATTERER
PLOT OF INCREASE IN RADIATION AS A FUNCTION OF SOURCE-DETECTOR SEPARATION AND A FUNCTION OF ATOMIC NUMBER "Z" DUE TO BACKSCATTERING FROM A SEMI-INFINITE SCATTERER IN CONTACT WITH THE SOURCE
Percent Increase in Radiation Due to Scattering
0
2
4
6
8
10
□ d = 5 cm
○ d = 10 cm
0
8
16
24
32
40
48
56
60
68
76
82
Atomic Number Z

Figure 9

quite large for photons below 400 kev. In lead the photons scattered into the chamber would be almost entirely of energies greater than 300-400 kev because lead is practically "opaque" to photons below this energy.

2. Back-scattering

The percentage increase in chamber current due to "back-scattering" is shown in Fig. 9. Since the minimum scattering angle for singly scattered photons to reach the detector is 90°, and the average angle is more nearly 180°, most of the scattered photons will have energies below 300 kev. At 180° the energy is down to 200 kev. All percentage increases should therefore be multiplied by a factor of about 1.1, because it is only the increase in chamber current due to scattering which is attenuated 10 percent as indicated by the frequency response characteristics of the chamber.

C. Interpretation of Results; Comparison with Scattering in an Infinite Medium

1. Side-scattering

The curves of Figs. 5, 6, 7, and 8 have the same general shape, except when the scattering medium is within about 1 cm of the source and detector, and resemble

quite large for photons below 400 kev. In lead the photons scattered into the chamber would be almost entirely of energies greater than 600-400 kev because lead is practically "opaque" to photons below this energy.

2. Back-scattering

The percentage increase in chamber current due to "back-scattering" is shown in Fig. 9. Since the minimum scattering angle for singly scattered photons to reach the detector is 90°, and the average angle is more nearly 180°, most of the scattered photons will have energies below 500 kev. At 180° the energy is down to 200 kev. All percentage increases should therefore be multiplied by a factor of about 1.1, because it is only the increase in chamber current due to scattering which is estimated in percent as indicated by the frequency response characteristics of the chamber.

c. Interpretation of Results; Comparison with Scattering in an Infinite Medium

1. Side-scattering

The curves of Figs. 5, 6, 7, and 8 have the same general shape, except when the scattering medium is within about 1 cm of the source and detector, and resemble

the build-up of scattered radiation obtained by VanDilla outside a water medium. A significant difference occurs at smaller distances, however, when the source-chamber separation in mean free paths becomes large. There is then a decrease in scattered radiation reaching the chamber because the photons which reach the chamber are traveling farther in the medium and have a greater probability of being multiply-scattered and of being absorbed by the photoelectric process. The shape of the curves is thus the result of two opposing effects. As the scattering material is brought closer the "illumination" of each volume element of scattering material becomes more intense and the illumination of the detector by the scattering volume becomes even more intense, because the distances between the volume element and both the source and the detector are decreasing. In addition, we see from Table III-1 that half of the photon energy of the singly-scattered Compton photons from each small volume element lies within a cone whose axis is along the direction of the primary radiation and whose vertex angle is about 70°. The detector intercepts more of the scattered energy as the scattering angles from a given volume element to the detector decrease due to this

the build-up of scattered radiation obtained by Padilla
outside a water medium. A significant difference oc-
curs at smaller distances, however, when the source-
chamber separation in mean free paths becomes large.
There is then a decrease in scattered radiation reaching
the chamber because the photons which reach the chamber
are traveling farther in the medium and have a greater
probability of being multiply-scattered and of being ab-
sorbed by the photoelectric process. The sum of the
curves is thus the result of two opposing effects. As
the scattering material is brought closer the "illumi-
nation" of each volume element of scattering material
becomes more intense and the illumination of the detec-
tor by the scattering volume becomes more intense,
because the distances between the volume element and
both the source and the detector are decreasing. In ad-
dition, we see from Table III-1 that half of the photon
energy of the singly-scattered Compton photons from each
small volume element lies within a cone whose axis is
along the direction of the primary radiation and whose
vertex angle is about 70°. The detector therefore sees
of the scattered energy as the scattering angles from a
given volume element to the detector decrease due to this

anisotropic angular distribution of scattered radiation. As the surface of the scattering material gets very close to the plane of the source and detector, however, a point is reached where these distances and angles are changing so slowly, and the path lengths in the medium increasing so rapidly, that the net illumination at the detector decreases if the attenuation in the medium is sufficiently severe. At d = 0 the paths of the scattered photons from a point source to a point detector would lie entirely in the medium. A chamber of finite size located entirely outside the medium will always detect some photons which are scattered near the surface of the medium and whose paths traverse very little of the medium. For this reason the experimental data obtained at small distances, d, will indicate a larger component of scattered radiation than would be obtained with a point detector.

Figure 10 shows the effect of varying the source-chamber separation when d is held constant at 2.5 cm. The primary radiation at the detector falls off with the inverse-square of the separation, s, as s increases; but the scattered radiation falls off less rapidly due to the anisotropy of the Compton-scattered photons. At d = 2.5 cm the increasing attenuation with path lengths

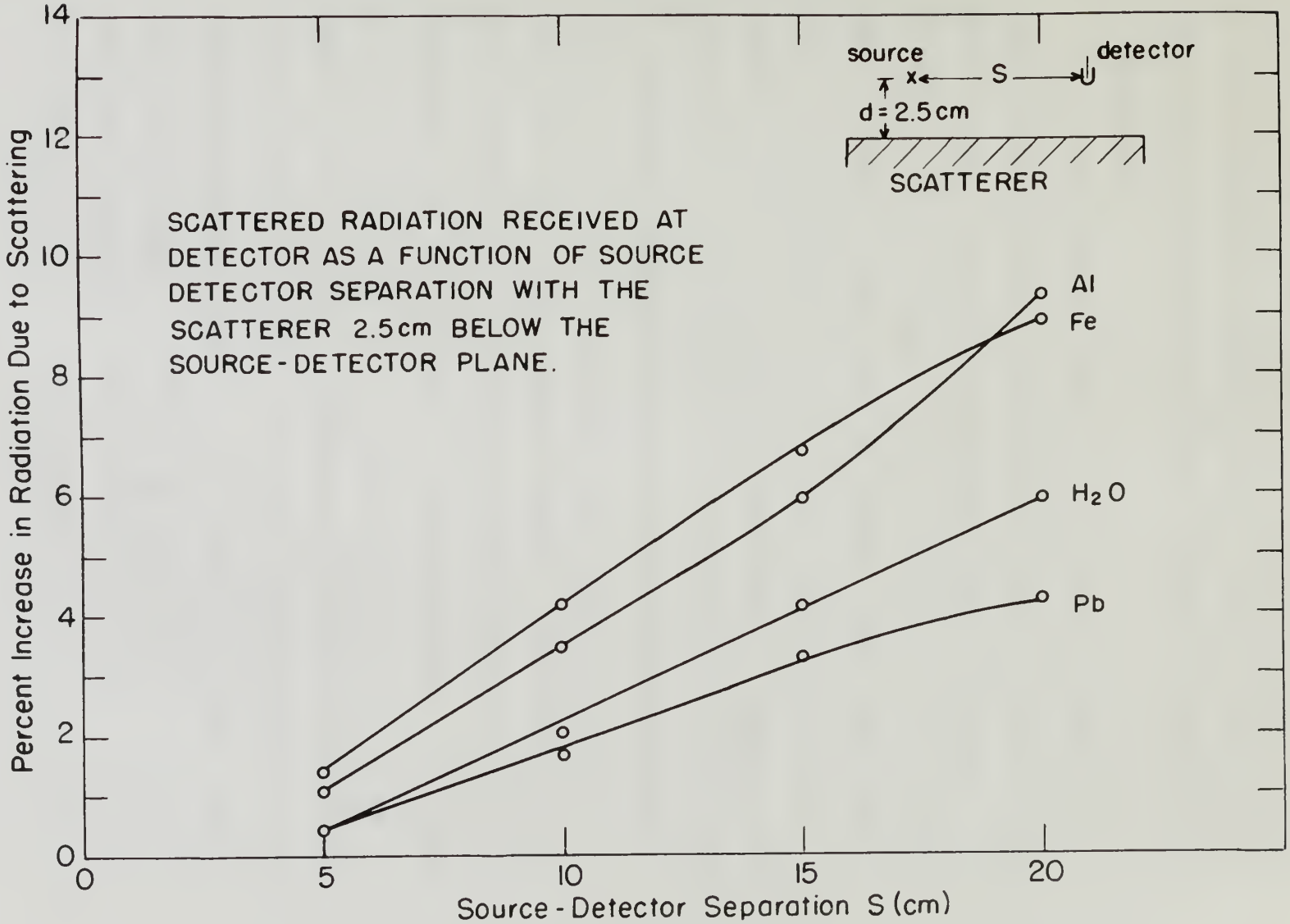
source
detector
x
S
d = 2.5 cm
SCATTERER
SCATTERED RADIATION RECEIVED AT DETECTOR AS A FUNCTION OF SOURCE DETECTOR SEPARATION WITH THE SCATTERER 2.5 cm BELOW THE SOURCE-DETECTOR PLANE.
Al
Fe
H_2O
Pb
Percent Increase in Radiation Due to Scattering
0
2
4
6
8
10
12
14
0
5
10
15
20
Source-Detector Separation S (cm)

Figure 10

in the medium never exceeds the "amplification" obtained as the scattering angles decrease, and all four materials yield an increased percent scattered radiation as s increases.

As the electron density increases from water to lead, there are more scattering centers per unit volume; and a larger fraction of scattered flux originates within a given distance from the surface of the medium. Both of these factors tend to increase the scattered flux at the detector for the same values of d and s. However, there is a greater attenuation of flux per unit path length in the medium due to multiple scattering and to photoelectric absorption, and the atomic cross-section for the latter increases with about the fourth power of Z at a given photon energy. The interplay of these factors is a complicated function of the nature of the medium and the geometry of the experiment. Figures 11 and 12 show that over a wide range of d and s the trend is an increased scattering with decreasing values of Z of the medium when Z is large and photoelectric absorption is appreciable. At low values of Z the trend reverses, because photoelectric absorption is becoming relatively unimportant and the mean free path for Compton scattering at a given photon energy is increasing

in the medium never exceeds the "amplification" obtained as the scattering angles decrease, and all four scattering yield an increased percent scattered radiation as $\underline{x}$ increases.

As the electron density increases from water to lead, there are more scattering centers per unit volume; and a larger fraction of scattered flux originates within a given distance from the surface of the medium. Both of these factors tend to increase the scattered flux at the detector for the same values of θ and $\underline{x}$. However, there is a greater attenuation of flux per unit path length in the medium due to multiple scattering and to photoelectric absorption, and the atomic structure-sensitive for the latter increases with about the fourth power of Z at a given photon energy. The interplay of these factors is a complicated function of the nature of the medium and the geometry of the experiment. Figures 11 and 12 show that over a wide range of θ and $\underline{x}$ the trend is an increased scattering with decreasing values of I of the medium even I is large for photoelectric absorption is appreciable. At low values of I the trend reverses, because photoelectric absorption is becoming relatively unimportant and the main free path for scattering at a given photon energy is increasing

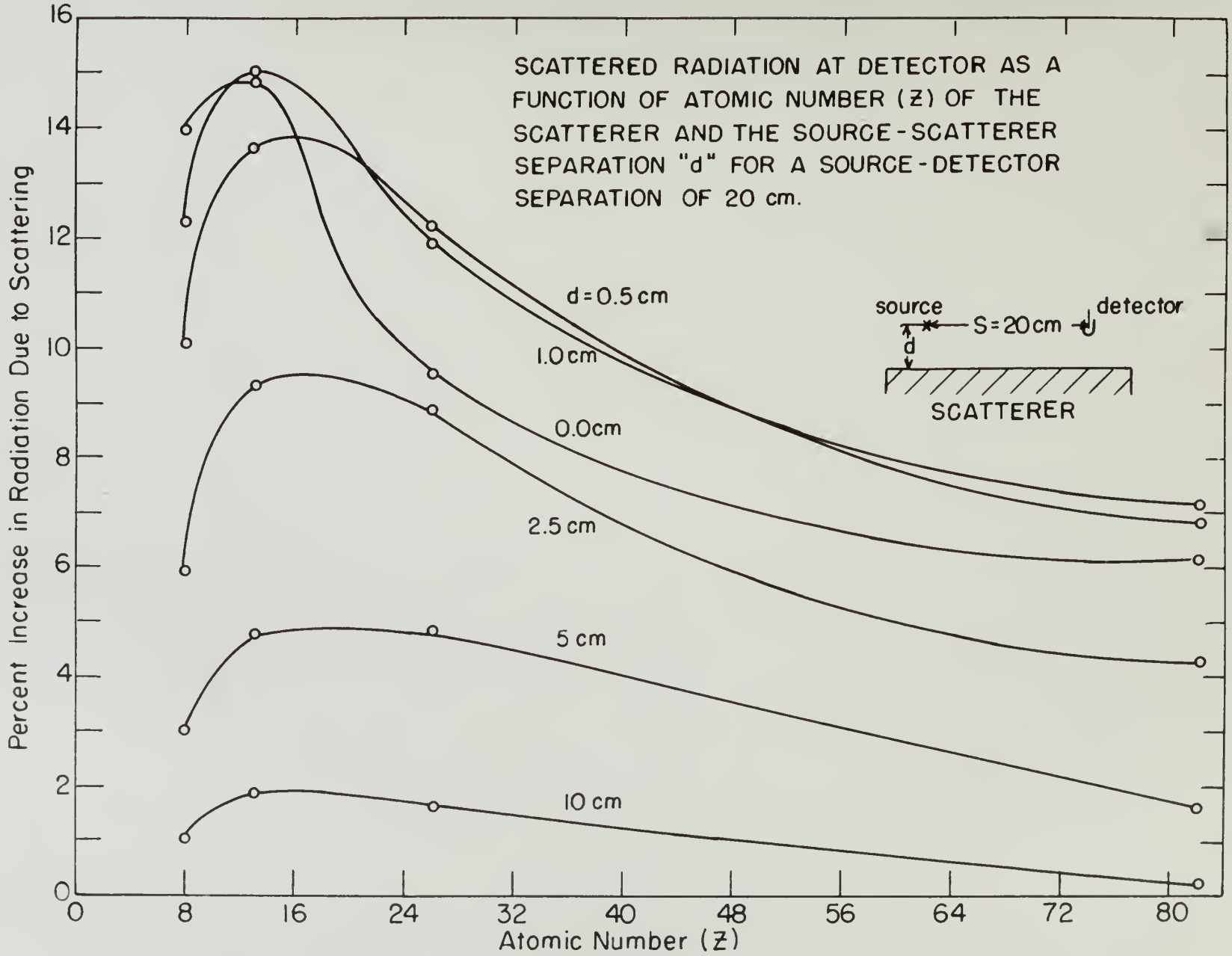
SCATTERED RADIATION AT DETECTOR AS A FUNCTION OF ATOMIC NUMBER (Z) OF THE SCATTERER AND THE SOURCE-SCATTERER SEPARATION "d" FOR A SOURCE-DETECTOR SEPARATION OF 20 cm.
d = 0.5 cm
1.0 cm
0.0 cm
2.5 cm
5 cm
10 cm
source
S = 20 cm
detector
d
SCATTERER
Percent Increase in Radiation Due to Scattering
Atomic Number (Z)
0
2
4
6
8
10
12
14
16
0
8
16
24
32
40
48
56
64
72
80

Figure 11

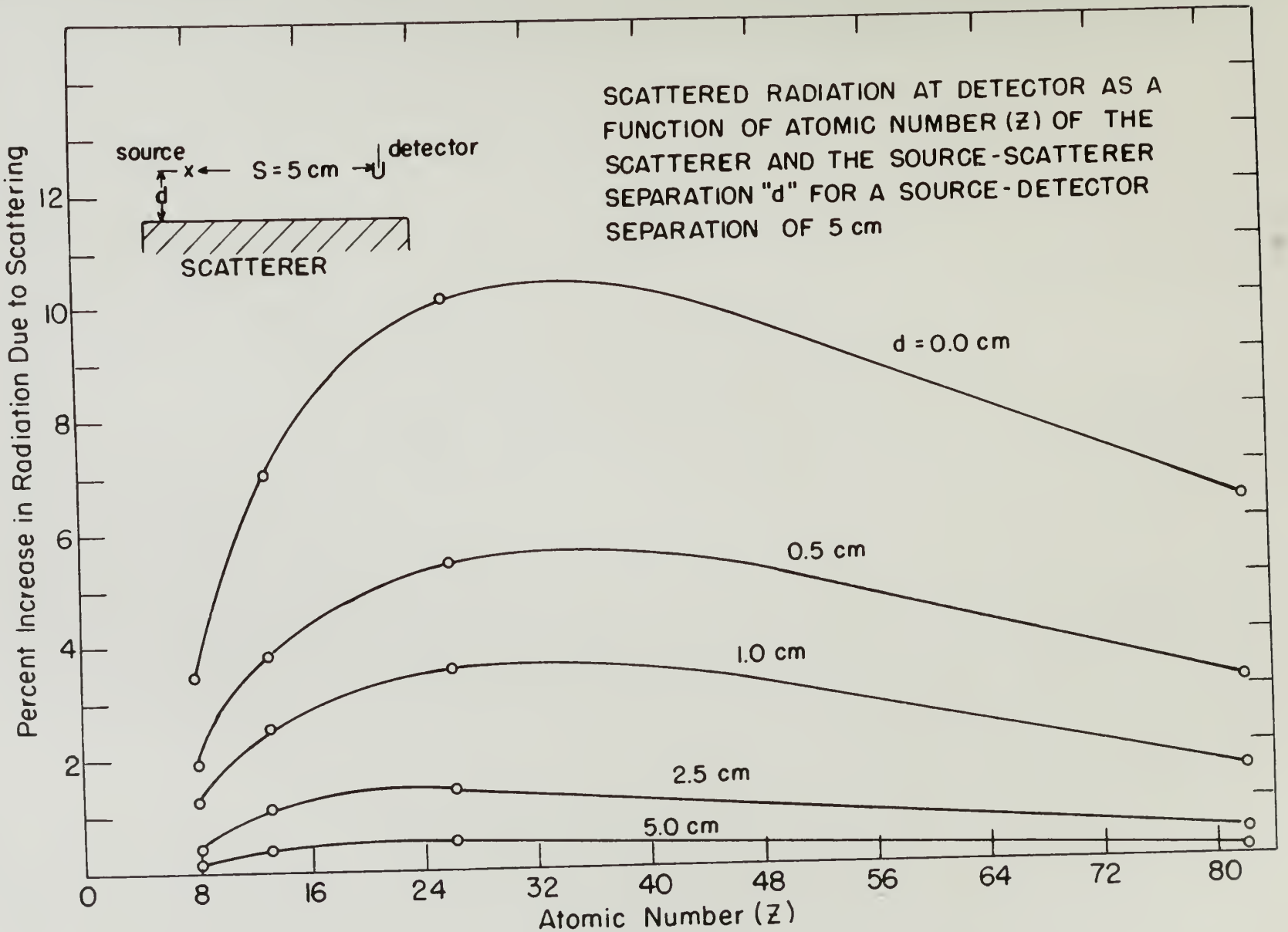
SCATTERED RADIATION AT DETECTOR AS A FUNCTION OF ATOMIC NUMBER (Z) OF THE SCATTERER AND THE SOURCE-SCATTERER SEPARATION "d" FOR A SOURCE-DETECTOR SEPARATION OF 5 cm
source
x
S = 5 cm
detector
d
SCATTERER
Percent Increase in Radiation Due to Scattering
0
2
4
6
8
10
12
d = 0.0 cm
0.5 cm
1.0 cm
2.5 cm
5.0 cm
0
8
16
24
32
40
48
56
64
72
80
Atomic Number (Z)

Figure 12

with the decreasing electron density. The inverse-square attenuation of illumination and the larger scattering angles which result when the photons that reach the chamber are scattered from points deeper in the medium tend to decrease the scattered flux at the detector as the electron density decreases.

In water the mean free path of primary photons from Co^{60} is 15.6 cm, while in aluminum it is 6.7 cm, so that roughly twice the thickness of material is required to approximate a semi-infinite medium of water as is required for aluminum. When $\underline{s}$ and $\underline{d}$ are small, the geometry of the experiment is changed more radically by the absolute magnitudes of the effective thickness of the scattering medium than when $\underline{s}$ and $\underline{d}$ are large.

Some information of practical value can be drawn from the results of the side-scattering experiments. A thin sheet of lead placed over a scattering medium of lower Z and appreciable thickness could be used to reduce scattering when the source and detector are not too close to the scattering medium. At large source-detector separations an aluminum collimator could be used to increase the dosage rate at the detector. At s = 20 cm an increase in dosage rate from Co^{60} of about 30 percent

would be obtained over a volume similar to that of our detector with collimator walls about 0.5 cm away from the sensitive volume.

As VanDilla has pointed out, with a point source and a point detector the increase in scattering of an infinite medium as compared with a semi-infinite medium will be due to two contributions: 1) the equal scattering contribution of the second half-infinite medium and 2) the contribution of scattering between the two half-infinite media. Figures 13 and 14 show the effect of using this idea to estimate build-up factor in an infinite medium when the source and detector geometries are rather broad, as they are in this experiment, especially near d = 0 where the attenuation is changing rapidly with small changes in angle.

The build-up factor is defined as $\frac{\text{total dosage rate}}{\text{primary dosage rate}}$. The build-up factor in aluminum was calculated from Evans'[27] analysis of Gray's[13] data. The BF as determined experimentally in water by VanDilla and by White[1] agree very well, and the recent theoretical calculations by Spencer and Fano[24] fit these data out to 16 mfp's, where the BF is about 33.8. The build-up factor is obtained from our data from the relation BF =

$1 + \frac{\text{percent increase}}{100} \times e^{\mu_o r} \times f$. The basis for this relation is that had the scattering medium been brought to a slightly negative distance (source inside the medium), the actual increase in chamber current would remain the same, but the percentage of increase would be based on the current measured in air $\times e^{-\mu_o r}$. The factor f is the ratio of the BF-1 in an infinite medium to the same quantity in a semi-infinite medium, and we would expect it to have a value somewhat larger than 2.

As indicated in Figs. 13 and 14 this concept gives fair agreement between the build-up factor in semi-infinite and infinite media at small source-chamber separations, where the effect of attentuation is small (up to about 1 mfp). At larger separations, however, the build-up factor for a semi-infinite medium, computed with f = constant, tends to approach an exponential. The behavior of the factor f as a function of source-chamber separation is also shown in Fig. 15. This figure shows conclusively that $f \neq$ constant, but in fact decreases continuously as the source-chamber separation increases, probably ultimately tending towards zero. Values of f less than 2 can be explained by consideration of the fact that Compton scattering is strongly anisotropic, with the greater scattering occurring

$1 + \frac{\text{percent increase}}{100} = e^{\mu_0 x}$ or f. The basis for this relation is that the scattering medium been removed to a slightly negative distance (source inside the medium), the actual increase in observer current would result, the same, but the percentage of increase would be based on the current measured in air $x e^{-\mu_0 x}$. The factor f is the ratio of the $\frac{1}{r^2}$-x in an infinite medium to the same quantity in a semi-infinite medium, and we would expect it to have a value somewhat larger than 1.

As indicated in Fig. 15 and in this concept gives fair agreement between the build-up factor in semi-infinite and infinite media at small source-observer separations, where the effect of attenuation is small (up to about μx). At larger separations, however, the build-up factor for a semi-infinite medium, compared with f = constant, tends to approach an exponential. The behavior of the factor f as a function of source-observer separation is also shown in Fig. 15. This figure shows numerically that f is constant, but in fact departures continuously as the source-observer separation increases, gradually diminishing towards zero. Values of f less than 1 can be explained by consideration of the fact that Compton scattering in

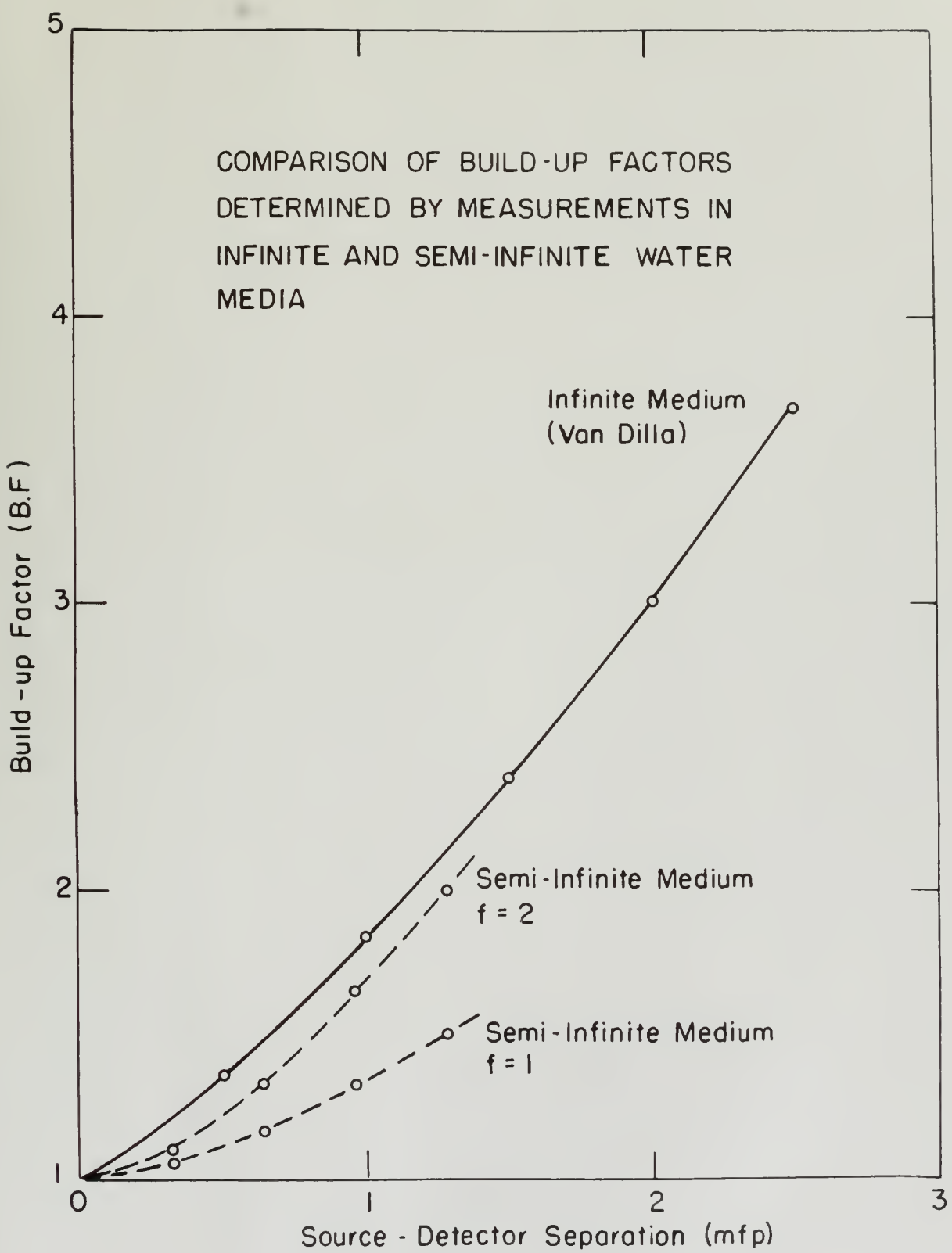
COMPARISON OF BUILD-UP FACTORS DETERMINED BY MEASUREMENTS IN INFINITE AND SEMI-INFINITE WATER MEDIA
Infinite Medium (Van Dilla)
Semi-Infinite Medium f = 2
Semi-Infinite Medium f = 1
Build-up Factor (B.F)
Source - Detector Separation (mfp)
0
1
2
3
4
5

Figure 13

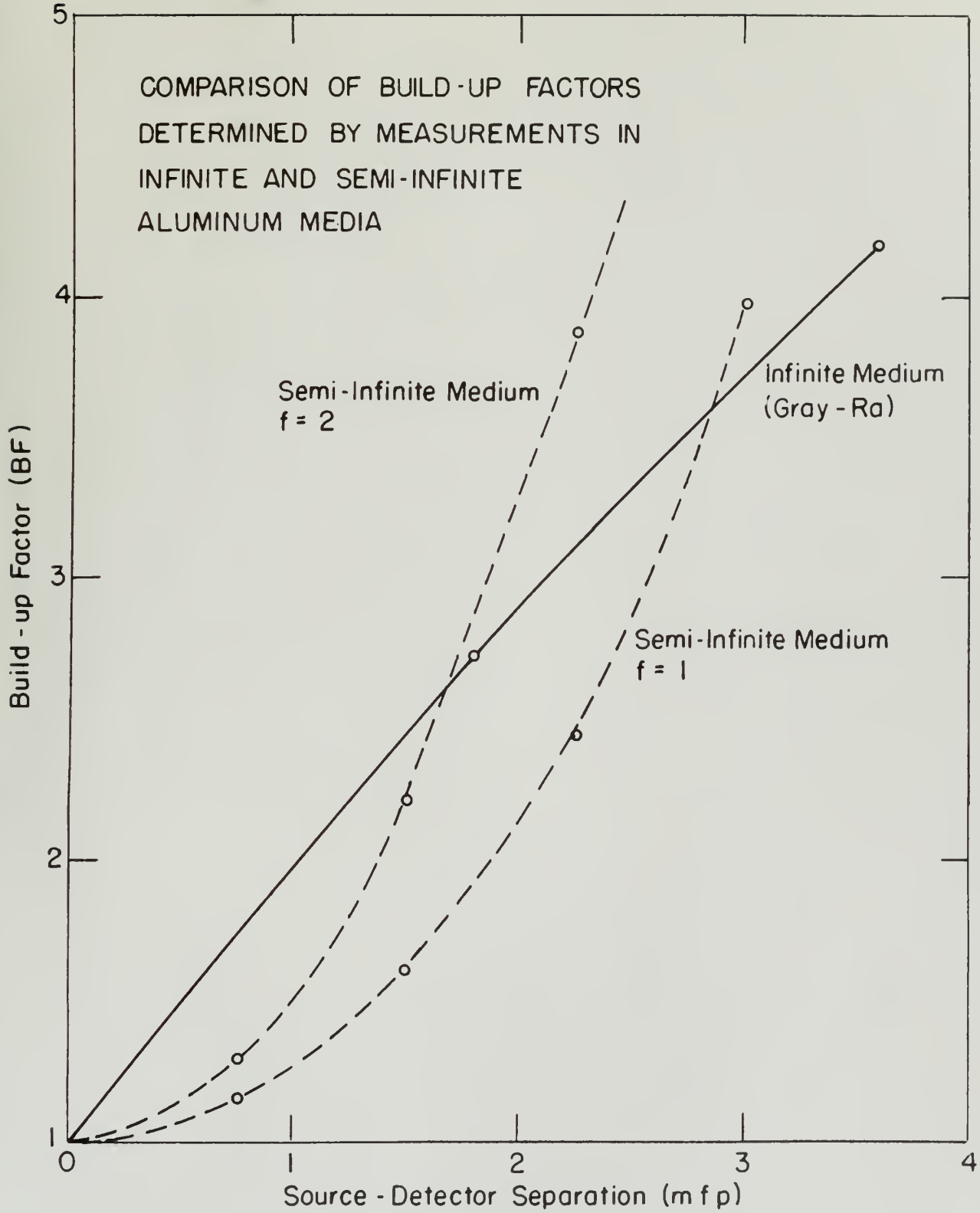
COMPARISON OF BUILD-UP FACTORS
DETERMINED BY MEASUREMENTS IN
INFINITE AND SEMI-INFINITE
ALUMINUM MEDIA
Semi-Infinite Medium
f = 2
Infinite Medium
(Gray - Ra)
Semi-Infinite Medium
f = 1
Build-up Factor (BF)
Source - Detector Separation (m f p)
0
1
2
3
4
5

Figure 14

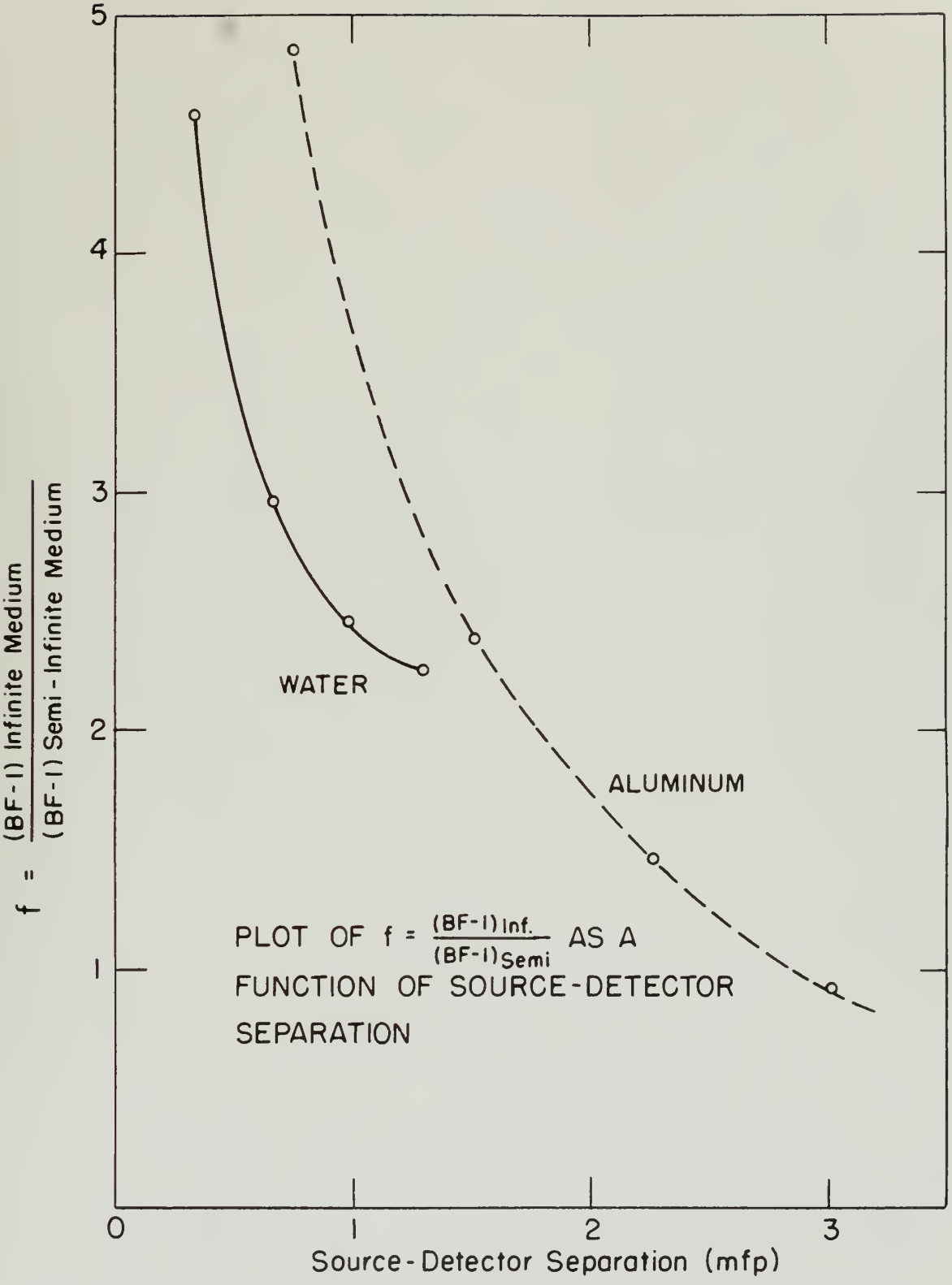
5
4
3
2
1
0
1
2
3
f = (BF-1) Infinite Medium / (BF-1) Semi-Infinite Medium
WATER
ALUMINUM
PLOT OF f = (BF-1)Inf. / (BF-1)Semi AS A FUNCTION OF SOURCE-DETECTOR SEPARATION
Source-Detector Separation (mfp)

Figure 15

at small angles in the forward direction. As the source-chamber distance is increased, this anisotropy results in a greater percentage of the scattered radiation reaching the detector after one or two small-angle scatterings near the surface of the medium. Consequently, a large part of the path length is in air and is no longer attenuated by the medium. The trend toward a vanishing value of f is thus due, primarily, to the finite size of the detector and is a complex function of the electron density of the medium and the solid angle subtended, at the source, by the detector. It can be corrected only by reducing the detector size. An ideal point source and point detector would not show this effect, since the paths of all scattered radiation reaching the detector would then lie wholly within the scattering medium. The large value of f at small source-chamber separations indicates the important contribution to total flux at the chamber by multiply-scattered photons. At small separations the major contributions are due to large-angle scattering. The absence of half of an infinite medium allows the escape of photons which might otherwise be detected by virtue of multiple scattering and hence multiple traversals of the detector.

versals of the detector.

virtue of multiple scattering and hence multiple tre-
escape of photons which might otherwise be detected by
The absence of half of an infinite medium allows the
major contributions are due to large-angle scattering.
tiply-scattered photons. At small separations the
tant contribution to total flux at the detector by mul-
small source-observer separations indicates the impor-
within the scattering medium. The large value of f at
radiation reaching the detector would then lie wholly
above this effect, since the paths of all scattered
An ideal point source and point detector would not
It can be corrected only by reducing the detector size.
to the finite size of the detector and is a complex
function of the electron density of the medium and the
solid angle subtended, at the source, by the detector.
toward a vanishing value of f is thus due, primarily,
and is no longer attenuated by the medium. The trend
sequently, a large part of the path length is in air
angle scatterings near the surface of the medium. Con-
tion reaching the detector after one or two small-
reaches in a greater percentage of the scattered radia-
source-observer distance is increased, this anisotropy
at small angles in the forward direction. As the

2. Back-scattering

The results of the back-scattering experiments indicate that the percent increase is relatively independent of geometry. This effect can be explained by considering that the majority of the scattered photons which strike the detector originate in a rather small region in the medium behind the source. The scattering angles of singly-scattered photons which reach the detector will lie between 90° and 180°. For these scattering angles the energies of the scattered photons are then mostly less than 300 kev. At these low energies the absorption and scattering cross-sections become quite large. In all cases material deeper than about one-half mean free path of the primary radiation will contribute essentially no additional detectable scattering at the detector. It is then possible, for qualitative visualization purposes, to conceive of an "image" source located in the medium directly behind the true source, and only a small fraction of a mean free path below the surface, from which the scattered radiation emanates. This "image" source is not, however, an image in the optical sense of the word since it does not reproduce exactly the position and frequency

2. Back-scattering

The results of the back-scattering experiments indicate that the present increase is relatively independent of geometry. This effect can be explained by considering that the majority of the scattered photons which strike the detector originate in a rather small region in the medium behind the source. The back-scattering angles of singly-scattered photons which reach the detector will lie between 90° and 180°. For these scattering angles the energies of the scattered photons are thus nearly less than 500 kev. At these low energies the absorption and scattering cross-sections become quite large. It will cause material deeper than about one-half mean free path at the primary radiation will contribute essentially no additional detectable scattering at the detector. It is then possible, for qualitative visualization purposes, to consider of an image source located in the medium directly behind the true source, and only a small fraction of a mean free path below the surface, from which the scattered radiation emanates. This image source is not, however, an image in the optical sense of the word since it does not reproduce exactly the position and intensity

characteristics of the source. It is, rather, a "pseudo-image" providing much lower frequency radiation (about 200-300 kev for a Co^{60} source) which is located at a distance below the surface which is small compared to a mean free path. The spectral characteristics are essentially independent of the scattering medium, but the location of the "image" source below the surface is an inverse function of atomic number Z and density ρ. For heavy (high Z and high ρ) materials the "image" source will be very near the surface, while for light materials (low Z and low ρ) it will lie a considerably greater distance below it.

With this concept it is possible to explain why the percent increase in radiation received at the detector is essentially independent of the source-chamber separation when the source is at the surface of the scattering medium. If the source-chamber separation is large compared with the separation between the true source and the image source, then both the primary radiation and the scattered radiation will show essentially the same attenuation due to the inverse-square effect.

The maximum at $Z \sim 13$ in Fig. 9 is due to the inclusion of measurements of backscattering from water.

Since from aluminum to water the mean free path of primary radiation increases 6.7 cm to 15.6 cm, the position of the image source has moved far enough into the medium so that inverse-square attenuation reverses the trend. Thus high Z materials do not allow the full potentiality of the medium for back-scattering to be realized, while materials with low electron density yield appreciable back-scattering contributions from greater distances below the surface of the medium. The variation of back-scattering with Z is the result of these two opposing effects.

ACKNOWLEDGMENTS

The authors are grateful to Professor Robley D. Evans for suggesting this project and for his helpful suggestions and criticisms in the preparation of this thesis, and to Dr. Gerald J. Hine who guided our efforts throughout the experimental work. We wish to thank all the other members of the Radioactivity Center who assisted in various ways by providing the facilities necessary to carry out the experimental work, as well as Mr. W. Kallenbach and the personnel of the Physics Work Shop, Mr. W. Ennis, Mr. E. J. Curtis, Mr. L. Coonrod, and Mr. R. Gustafson. Also a special note of thanks goes to Mrs. Grace Rowe for the drafting work.

ACKNOWLEDGMENTS

The authors are grateful to Professor Dudley C. Evans for suggesting this project and for his helpful suggestions and criticisms in the preparation of this thesis, and to Dr. Gerald I. Kerley who guided our efforts throughout the experimental work. We also to thank all the other members of the Geological Society Center who assisted in various ways by providing the facilities necessary to carry out the experimental work, as well as Dr. W. Tallmadge and the personnel of the Physics Data Shop, Mr. E. Smale, Mr. C. J. Curtis, Mr. L. Conrad, and Mr. T. Danielson. Also a special note of thanks goes to Mrs. Frona Rose for her dedicated work.

BIBLIOGRAPHY

1. G. R. White, Phys. Rev. 80, 184 (1950).
2. M. A. VanDilla, Ph.D. Thesis, MIT (1951).
3. L. H. Gray, Proc. Roy. Soc. (London) A159, 263 (1937).
4. Palvesky, Swank and Grenchik, R.S.I. 18, 298 (1947).
5. G. W. C. Kaye and W. Binks, Proc. Roy. Soc. (London) A161, 564 (1937).
6. L. S. Taylor, Brit. J. Rad. 24, 67 (1951).
7. W. H. Bragg, "Studies in Radioactivity", p. 92 et seq. (1912).
8. L. H. Gray, Proc. Roy. Soc. (London) A156, 578 (1936).
9. W. V. Mayneord and J. E. Roberts, Brit J. Rad. 10, 365 (1937).
10. C. Goodman, "The Science and Engineering of Nuclear Power", Addison-Wesley (Cambridge, 1947) p. 55.
11. D. E. Lea, Proc. Camb. Phil. Soc. 30, 80 (1934).
12. G. Jaffe, Ann. Physik 42, 303 (1913).
13. R. D. Evans, "Introduction to the Atomic Nucleus", MIT course notes (unpublished).
14. G. Holte, Arkiv för Fysik, Band 3, Häfte 1-3, 209 (1951).
15. C. M. Davisson, Ph.D. Thesis, MIT (1948).
16. L. F. Lamerton, Brit. J. Rad. 21, 276 (1948).
17. Hirschfelder, Magee and Hull, Phys. Rev. 73, 852 (1948).
18. J. Hirschfelder and E. Adams, Phys. Rev. 73, 863 (1948).

BIBLIOGRAPHY

1. G. S. Hoyle, Phys. Rev. 50, 124 (1936).

2. R. A. Ventrella, Ph.D. Thesis, ECT (1952).

3. L. D. Orey, Proc. Soc. Exp. Biol. (London) 117, 203 (1957).

4. Privately, Evans and Creecraft, I.E.I. 16, 294 (1947).

5. G. H. C. Kaye and T. Price, Proc. Roy. Soc. (London) A143, 565 (1937).

6. L. S. Taylor, Phil. J. Med. 24, 47 (1941).

7. W. Dreyer, "Absolute Radiometrist", p. 95 et seq. (1912).

8. L. E. Orel, Typoc. Soy. Inc. (London) A156, 578 (1936).

9. G. T. Kapitzand and T. S. Gleaves, Brit. J. Med. 10, 765 (1937).

10. C. Darwin, "The Science and Beginning of Nuclear Power", Addison-Wesley (Reading, 1947) p. 6.

12. D. S. Lee, Typo. Chem. Phil. Soc. 20, 60 (1934).

13. C. Price, Amer. Physik 45, 305 (1915).

15. E. D. Trent, "Instruction by the Atomic Industry", ELI course notes (unpublished).

14. D. Wolfe, Irely Int Typic, Head ", Wolfe L-3, 207 (1936).

16. C. M. Peterson, Ph.D. Thesis, ECT (1944).

16. E. Lawrence, Math. J. Phil. 27, 176 (1946).

17. Ferrocyanides, Sayre and Wall, Chem. Inc. 70, 200 (1948).

18. Electrochemistry and L. Adams, Phys. Inc. 72, 845 (1949).

19. M. S. Plesset and S. T. Cohen, J. Appl. Phys. 22, 350 (1951).

20. U. Fano and P. R. Karr, Phys. Rev. 75, 1303 A5 (1949).

21. U. Fano, Phys. Rev. 76, 739 (1949).

22. Bethe, Fano and Karr, Phys. Rev. 76, 538 (1949).

23. P. R. Karr and J. C. Lamkin, Phys. Rev. 76, 1843 (1949).

24. L. V. Spencer and U. Fano, Phys. Rev. 81, 464 L (1951).

25. L. L. Foldy and R. K. Osborn, Phys. Rev. 81, 400 (1951).

26. W. R. Faust, Phys. Rev. 77, 227 (1950).

27. R. D. Evans, "Advances in Biological and Medical Physics", Academic Press, Inc. (New York, 1948) Vol I.

19. W. E. Pleasod and E. I. Colman, J. appl. Phys. 12, 880 (1941).

20. B. Yang and P. M. Eaur, Phys. Rev. 73, 1504 A3 (1948).

21. U. Fano, Phys. Rev. 70, 780 (1946).

22. Beutler, Fano and Eaur, Phys. Rev. 70, 638 (1946).

23. E. E. Barr and J. C. Lambkin, Phys. Rev. 70, 1946 (1946).

24. E. T. Bowmore and O. Thom, Proc. Phys. Soc. 61, 494 L (1951).

25. C. T. Tolly and R. E. Osborn, Phys. Rev. 81, 400 (1951).

26. R. N. Peuse, Phys. Rev. 77, 234 (1950).

27. B. O. Evans, "Advances in Nuclear and Neutral Physics", Academic Press, Inc. (New York, 1949) Vol I.

OCT 2 BINDERY

18067

Thesis W553 White
Measurements of gamma-ray scattering using a liquid-filled ionization..

OCT 2 BINDERY

18067

Thesis W553 White
Measurements of gamma-ray scattering using a liquid-filled ionization chamber. . . .

Library
U. S. Naval Postgraduate School
Monterey, California

thesW553
Measurements of gamma-ray scattering usi
3 2768 001 95065 2
DUDLEY KNOX LIBRARY